AMERICAN SOCIETY FOR MICROBIOLOGY | Infection and Immunity

Transcriptional Profiling of *Mycobacterium tuberculosis* Exposed to *In Vitro* Lysosomal Stress

Wenwei Lin,[a,b,c]* Paola Florez de Sessions,[d] Garrett Hor Keong Teoh,[d] Ahmad Naim Nazri Mohamed,[d] Yuan O. Zhu,[d] Vanessa Hui Qi Koh,[a,b] Michelle Lay Teng Ang,[a,b]* Peter C. Dedon,[c] Martin Lloyd Hibberd,[d,e] Sylvie Alonso[a,b,c]

Department of Microbiology and Immunology, Yong Loo Lin School of Medicine, National University of Singapore, Singapore[a]; Immunology Programme, Life Sciences Institute, National University of Singapore, Singapore[b]; Infectious Disease Interdisciplinary Research Group, Singapore-MIT Alliance for Research and Technology, Singapore[c]; Genome Institute of Singapore, Agency for Science, Technology and Research, Singapore[d]; Department of Pathogen Molecular Biology, London School of Hygiene & Tropical Medicine, London, United Kingdom[e]

Increasing experimental evidence supports the idea that *Mycobacterium tuberculosis* has evolved strategies to survive within lysosomes of activated macrophages. To further our knowledge of *M. tuberculosis* response to the hostile lysosomal environment, we profiled the global transcriptional activity of *M. tuberculosis* when exposed to the lysosomal soluble fraction (SF) prepared from activated macrophages. Transcriptome sequencing (RNA-seq) analysis was performed using various incubation conditions, ranging from noninhibitory to cidal based on the mycobacterial replication or killing profile. Under inhibitory conditions that led to the absence of apparent mycobacterial replication, *M. tuberculosis* expressed a unique transcriptome with modulation of genes involved in general stress response, metabolic reprogramming, respiration, oxidative stress, dormancy response, and virulence. The transcription pattern also indicates characteristic cell wall remodeling with the possible outcomes of increased infectivity, intrinsic resistance to antibiotics, and subversion of the host immune system. Among the lysosome-specific responses, we identified the *glgE*-mediated 1,4 α-glucan synthesis pathway and a defined group of VapBC toxin/anti-toxin systems, both of which represent toxicity mechanisms that potentially can be exploited for killing intracellular mycobacteria. A meta-analysis including previously reported transcriptomic studies in macrophage infection and *in vitro* stress models was conducted to identify overlapping and nonoverlapping pathways. Finally, the Tap efflux pump-encoding gene *Rv1258c* was selected for validation. An *M. tuberculosis* Δ*Rv1258c* mutant was constructed and displayed increased susceptibility to killing by lysosomal SF and the antimicrobial peptide LL-37, as well as attenuated survival in primary murine macrophages and human macrophage cell line THP-1.

Mycobacterium tuberculosis infects a third of the world's population and causes death to millions of infected individuals annually. While 90% of the infected population is able to prevent progression into active disease, incomplete sterilization of the infecting bacilli, typically within granulomatous lesions formed in the lungs, leads to latent tuberculosis (TB), the asymptomatic form of the disease. It is a longstanding paradigm that these lesions provide a niche environment that induces TB latency, where the bacterium is believed to enter a state of bacteriostasis or very slow replication with low energetic and metabolic activities and retains the ability to resume growth under permissive conditions, leading to disease reactivation (1).

Macrophages represent a large proportion of the cell populations that are present in a TB lung granuloma (2, 3). Their phagocytic abilities are responsible for eliminating most intracellular microbes, and as such macrophages are important players in host innate immunity (4, 5). However, upon phagocytosis, internalized *M. tuberculosis* is able to survive and replicate within the phagosome by blocking its fusion with lysosomes according to a process that involves several mycobacterial lipid and protein factors (6). Following the onset of cell-mediated immunity, however, macrophage activation overrides phagosome maturation arrest and delivers *M. tuberculosis* into the lysosomal compartment (7, 8), characterized by an increased acidic environment and containing a plethora of bactericidal molecules, including hydrolytic enzymes, oxygenated lipids, fatty acids, reactive oxygen species and nitrogen intermediates, and antimicrobial peptides. However, killing of mycobacteria in activated macrophages appears to be a protracted event, as evidenced by the detection of low numbers of viable bacilli 7 days postinfection (7, 8). With an increasing number of mycobacterial factors reported to be specifically implicated in *M. tuberculosis* survival within activated macrophages (9), it seems that this pathogen has evolved strategies to adapt and survive within this hostile compartment, thereby challenging the idea that the lysosomal compartment is a dead end for *M. tuberculosis*. Specific *M. tuberculosis* responses to the lysosomal environment could therefore be exploited to identify novel targets and develop

Received 24 January 2016 **Returned for modification** 12 February 2016
Accepted 10 June 2016

Accepted manuscript posted online 20 June 2016

Citation Lin W, de Sessions PF, Teoh GHK, Mohamed ANN, Zhu YO, Koh VHQ, Ang MLT, Dedon PC, Hibberd ML, Alonso S. 2016. Transcriptional profiling of *Mycobacterium tuberculosis* exposed to *in vitro* lysosomal stress. Infect Immun 84:2505–2523. doi:10.1128/IAI.00072-16.

Editor: S. Ehrt, Weill Cornell Medical College

Address correspondence to Sylvie Alonso, micas@nus.edu.sg.

* Present address: Wenwei Lin, Singapore Programme of Research Investigating New Approaches to Treatment of Tuberculosis (SPRINT-TB), Yong Loo Lin School of Medicine, National University of Singapore (NUS), Singapore; Michelle Lay Teng Ang, Lee Kong Chian School of Medicine and School of Biological Sciences, Nanyang Technological University, Singapore.

Supplemental material for this article may be found at http://dx.doi.org/10.1128/IAI.00072-16.

novel anti-TB drugs. However, there is limited knowledge on the behavior and physiology of *M. tuberculosis* in the lysosomal compartment.

Transcriptional profiling of *M. tuberculosis* from infected macrophages of human or mouse origin has been the typical approach to decipher the behavior of intramacrophage *M. tuberculosis* (10–15). A comparative study between resting and gamma interferon (IFN-γ)-activated macrophages identified a specific subset of mycobacterial genes that were distinctly modulated in activated macrophages, thereby supporting a lysosome-specific transcriptional reprogramming in *M. tuberculosis* with the potential to adapt to the inhospitable lysosomal microenvironment (11). While these studies have captured dynamic global transcriptional changes in *M. tuberculosis* during macrophage infection, contradictory observations were also reported, likely due to underlying experimental differences between these macrophage infection models, for instance, the macrophage type and *M. tuberculosis* strains employed and/or the time postinfection at which the transcriptome was assessed. The unsynchronized infection process throughout the macrophage population could generate a transcriptional profile representative of a combination of *M. tuberculosis* gene responses to multiple microenvironments encountered during macrophage infection which prevent the dissection of responses pertaining to each of the subcellular environmental niches encountered by *M. tuberculosis* during its intramacrophage life. To address these limitations, gene expression studies have been conducted in defined *in vitro* culture settings that feature one particular stress or growth condition possibly encountered by *M. tuberculosis* during macrophage infection, including hypoxia (16), nitric oxide (17, 18), iron limitation (19), acidic pH (20), gradual oxygen depletion (21, 22), nutrient starvation (23, 24), antibiotic pressure (25), and stationary phase (26). These studies have allowed the identification of *M. tuberculosis* genes that respond specifically to a particular environmental cue or growth condition.

Our work aims to study the transcriptional response of *M. tuberculosis* to the lysosomal content using RNA sequencing (RNA-seq). *M. tuberculosis* was exposed to the lysosomal soluble fraction (SF) prepared from activated macrophages. Previous work has shown that the lysosomal SF possesses mycobactericidal activity in a dose- and time-dependent manner (27). Here, upon exposure to SF conditions that led to an absence of apparent mycobacterial replication, we report a unique transcriptional signature as part of *M. tuberculosis* adaptive response to the hostile lysosomal environment.

MATERIALS AND METHODS

Ethics statement. All of the animal experiments were carried out under the guidelines of the National Advisory Committee for Laboratory Animal Research (NACLAR) in the AAALAC-accredited NUS animal facilities (http://nus.edu.sg/iacuc/). NUS has obtained a license (VR008) from the governing body Agri-Food & Veterinary Authority of Singapore (AVA) to operate an Animal Research Facility. The animal experiments described in this work were approved by the IACUC from the National University of Singapore under protocol number R2014-00723.

Bacterial strains and growth conditions. The parental strain of *M. tuberculosis* CDC1551, its derived mutant, and complemented strains were grown in Middlebrook 7H9 medium (Difco) supplemented with 10% ADS [50 g bovine fraction V albumin, 20 g D-(+)-glucose, 8.1 g sodium chloride per liter], 0.05% Tween 80, and 0.5% glycerol or on Middlebrook 7H11 agar containing oleic acid-albumin-dextrose-catalase (OADC; Becton Dickinson) and 0.5% glycerol. When appropriate, hygromycin and kanamycin were added at 80 and 20 μg/ml, respectively. Hygromycin was purchased from Roche. Kanamycin, streptomycin, and carbonyl cyanide *m*-chlorophenyl hydrazone (CCCP) were purchased from Sigma. For CFU enumeration, serial dilutions were performed in the Middlebrook 7H9 medium and plated on Middlebrook 7H11 agar. Plates were incubated at 37°C for 3 to 4 weeks.

Determination of the MIC of streptomycin. Mid-log-phase mycobacterial cultures were grown in 7H9 medium and diluted to an optical density at 600 nm (OD_{600}) of 0.02. The diluted bacterial suspension (200 μl) was added to 2-fold serially diluted streptomycin (5 μl) in a flat-bottom 96-well plate and incubated for 5 days. The OD_{600} of the cultures were measured using a Bio-Rad iMark microplate absorbance reader at 600 nm. The values were plotted against the log concentrations of streptomycin, and a sigmoidal dose-response curve was fitted to the plot. The MIC corresponded to the concentration which inhibits 100% of visible bacterial growth based on the OD_{600}.

Extraction of lysosomal SF. The lysosomal soluble fractions (SF) were extracted from activated bone marrow-derived macrophages (BMMOs) as previously described (27). T75 flasks of confluent BMMOs were incubated for 2 h at 37°C and 5% CO_2 with 5 ml of 40 mg/ml iron-dextran (40 kDa) mixed with 2× Opti-MEM (Gibco) at a 1:1 ratio. The monolayers were rinsed twice in 10 ml of warmed sterile phosphate-buffered saline (PBS) to remove the excess Fe-dextran and chased overnight in culture medium. The cells were scraped in 5 ml of homogenization buffer (HB) (250 mM sucrose, 0.5 mM EGTA, 0.1% gelatin, and 20 mM Tris, pH 7.0), centrifuged at 1,500 rpm at 4°C for 10 min, and lysed by passing through a tuberculin syringe. The lysate was subjected to low-speed centrifugation at 1,000 rpm at 4°C for 10 min to remove debris, nuclei, and intact cells. The supernatant was applied to a MiniMACS column (Miltenyi Biotech) placed on a magnetic stand to retain the iron-loaded lysosomes. After two washes with HB, the column was removed from the magnetic stand, and the bound iron-loaded lysosomes were eluted twice with 500 μl of HB. The lysosomes were spun down at 12,000 rpm for 30 min and stored as a dry pellet at −20°C until use. To prepare the lysosomal SF, each pellet was resuspended in 200 μl of SF buffer (1% Tween 20, 20 mM sodium acetate, pH 5.5). The lysates from eight pellets (2.5×10^8 cells) were pooled and applied to two MidiMACS (Miltenyi Biotech) columns to remove iron. The flowthrough was collected and centrifuged at 100,000 rpm at 4°C for 50 min. The supernatant corresponding to the SF was collected and the total protein content was estimated using the bicinchoninic acid (BCA) protein assay kit (Thermo-Scientific Pierce). SF was stored at −80°C until use.

Bactericidal assays. Bactericidal assays on *M. tuberculosis* strains were performed with SF and synthetic human cathelicidin (LL-37; Peptide Institute, Japan). LL-37 was reconstituted in 0.01% acetic acid for storage in −80°C until use. When required, 1 μg/ml CCCP was added to the medium. Mid-log-phase mycobacterial cultures of 5×10^5 CFU/ml were treated with the indicated concentrations of the bactericidal agents for the indicated periods of time. The number of surviving bacteria was enumerated by plating appropriate dilutions of the mixture on 7H11 agar and incubating at 37°C for 3 weeks.

RNA isolation and qualitative real-time PCR. Mycobacterial cultures were incubated with RNAprotect bacterial reagent (Qiagen) for RNA stabilization. The pelleted bacteria were then resuspended in 100 μl Tris-EDTA (TE) containing 20 μg/ml lysozyme and incubated at room temperature for 20 min. RNA extraction was then performed using an RNeasy minikit (Qiagen) according to the manufacturer's instructions. Contaminating genomic DNA from the eluted total RNA was removed using the Turbo DNA-free kit according to the manufacturer's protocol. The RNA concentrations and purity were measured using a NanoDrop 1000 spectrophotometer (Thermo Scientific). Reverse transcription was performed on 10 ng bacterial RNA using the iScript cDNA synthesis kit (Bio-Rad). Real-time PCR was performed in a 96-well plate with each well containing 2 μl cDNA mix, 0.5 μl forward (F) and reverse (R) primers (0.5 μM final), and 25 μl SYBR green supermix with ROX (Bio-Rad) to a final volume of

50 μl. The list of primers is presented in Table S7 in the supplemental material. Samples were run in triplicate. Real-time PCR amplification was conducted with the ABI Prism 7500 sequence detector (Applied Biosystems) over 40 cycles and with an annealing temperature of 61°C. The expression of each target gene was based on relative quantification (RQ) using the comparative critical threshold (C_T) value method. Relative quantification of a specific gene was evaluated in each reaction by normalization to the C_T value obtained for the endogenous control gene, *sigA*. For validation of transcriptome sequencing (RNA-seq) data, fold changes (RQ values) were derived with reference to expression levels from *M. tuberculosis* incubated with SF buffer for 48 h. For validation of *Rv1258c* overexpression, the fold change was derived with reference to expression from WT *M. tuberculosis*.

RNA-seq library preparation. Total DNA-free RNA sample was depleted of bacteria rRNA with Ambion's MICROBExpress kit (AM1905) per the manufacturer's instructions. Bacterial rRNA-depleted sample was processed using the TruSeq RNA sample preparation (v2) per the manufacturer's instructions. Library preparation entailed fragmentation, 1st- and 2nd-strand cDNA synthesis, end repair, A tailing, and ligation of adapters with multiplex indexes according to the manufacturer's instructions. Samples were enriched with 15 PCR cycles followed by Agencourt AMPure XP magnetic bead (Beckman Coulter, Brea, CA, USA) clean up according to the manufacturer's instructions. The quality of cDNA libraries was checked with Agilent DNA1000 chips (2100 Bioanalyzer; Agilent Technologies, Santa Clara, CA, USA). Next-generation sequencing was performed using an Illumina HiSeq 2000 flow cell with two 76-bp end runs. PhiX was used as a control.

RNA-seq data analysis. RNA-seq data analysis was performed on the CLC Genomics platform. Sequence reads were aligned to the *Mycobacterium tuberculosis* CDC1551 parental reference genome (GenBank accession number NC_002755). The reads per kilobase per million (RPKM) value for each gene was generated. Differential gene expression analysis using the R edgeR package was performed for the following groups of data sets: incubation for 24 h or 48 h at 0, 10, or 20 μg/ml SF. The exact-test function was applied to determine the association of the differences in expression read counts within each group, and corresponding *P* values were adjusted using the default Benjamini & Hochberg procedure. Their adjusted *P* values, in $-\log_{10}$ scale on the *y* axis and fold changes in $\log_2$ scale on the *x* axis, were plotted as a volcano plot. Differential gene expression was determined by a false discovery rate (FDR) of <0.01. Genes with read counts of less than 5 from both SF-treated and nontreated groups were also eliminated. Further functional annotation clustering analysis was performed using Database for Annotation, Visualization and Integrated Discovery (DAVID), version 6.7 (28, 29), and TB Database (http://www.tbdb.org/).

Meta-analysis with *in vitro* and *ex vivo* models of *M. tuberculosis*. Microarray-based transcriptome studies of *M. tuberculosis* in *in vitro* and *ex vivo* models of *M. tuberculosis* were selected for comparative analysis with the *M. tuberculosis* transcriptome generated in this study. For short-term primary murine macrophage (BMMO) (10, 11) and human macrophage (THP-1) infection studies (13), genes that were differentially expressed at 24 h or 48 h after infection were considered. For temporal studies based on BMMO (30), genes that exhibited significant temporal trends were considered. For analysis with *in vitro* models of *M. tuberculosis* persistence, differential *M. tuberculosis* transcriptomes generated from gradual hypoxic (21), defined hypoxic (22), nutrient starvation (24) and drug-tolerant persister (25) models were considered.

Construction of Δ*Rv1258c* mutant and Ox-*Rv1258c* complemented strains. The Δ*Rv1258c* mutant strain was generated in the *M. tuberculosis* CDC1551 background by allelic exchange using the suicide plasmid backbone pYUB854, as previously described (31). Briefly, primers with relevant restriction enzyme sites (see Table S7 in the supplemental material) were designed to amplify 5′ and 3′ PCR fragments (~1 kb) flanking the *Rv1258c* open reading frame (ORF) from genomic DNA of the *M. tuberculosis* CDC1551 parental strain. The fragments were cloned into the pYUB854 plasmid at its corresponding multiple cloning sites (MCS) flanking the hygromycin resistance gene, *hyg*. A PacI-restricted fragment containing the selection genes *lacZ* and *sacB* was obtained from pGOAL17 (32) and cloned into the pYUB854-PCR5′-3′ construct to obtain the final delivery vector, pYUB854-*Rv1258c*. The overexpressing complemented strain Ox-*Rv1258c* was constructed by introducing *Rv1258c*, under the strong constitutive mycobacterial *hsp60* promoter, into the Δ*Rv1258c* mutant strain using a promoter-less integrative plasmid, pMV306 (33). The mycobacterial *hsp60* promoter was excised from pMV262 and cloned into MCS of pMV306 vector. The ORF of *Rv1258c* was amplified from *M. tuberculosis* CDC1551 parental genomic DNA using primers indicated in Table S7 and subsequently were inserted downstream of the *hsp60* promoter to obtain the final delivery vector, pMV306-*Rv1258c*. The UV-irradiated plasmid solutions (1 μg) were electroporated into the respective *M. tuberculosis* strains as described previously (32). To identify the Δ*Rv1258c* mutant, hygromycin-resistant white colonies were selected. Deletion at the *Rv1258c* locus was verified by PCR using primers listed in Table S7 and Southern blot analysis. To identify the Ox-*Rv1258c* strain, kanamycin-resistant colonies were selected. Quantitative reverse transcription-PCR (qRT-PCR) was used to detect increased transcriptional activity of *Rv1258c*.

Southern blot analysis. Chromosomal DNA (1 μg) prepared from each *M. tuberculosis* strain was digested with EcoRI and XmaI for 4 h and subjected to 0.8% agarose gel electrophoresis. The agarose gel containing the digested DNA was chemically treated and transferred onto a nitrocellulose membrane (Millipore) according to Roche's digoxigenin (DIG) application manual. The membrane was UV fixed for 1 min and equilibrated with 10 ml preheated DIG Easy Hyb solution (Roche) at 65°C for 20 min, with gentle agitation. A DIG-labeled probe was amplified using the PCR DIG probe synthesis kit (Roche) according to the manufacturer's instructions and primers as listed in Table S7. For hybridization, about 5 to 25 ng/ml heat-denatured DIG-labeled DNA probe in DIG Easy Hyb solution was incubated with the membrane overnight at 65°C. Detection was performed using alkaline phosphatase (AP)-conjugated anti-DIG antibody (Roche) at a dilution of 1:5,000. The membrane was developed using nitroblue tetrazolium–5-bromo-4-chloro-3-indolylphosphate (NBT-BCIP)-AP substrate (Chemicon).

Macrophage survival assays. Bone marrow cells were flushed from femurs of 6- to 8-week-old BALB/c mice, seeded onto petri dishes (4 femurs per dish; Greiner), and differentiated into macrophages over 6 days in BMMO complete medium supplemented with 10 ng/ml recombinant mouse macrophage colony-stimulating factor (rM-CSF; R&D Systems). Differentiated macrophages were recovered by dislodging them in cold 1× PBS containing 1 mM EDTA (pH 7.4) and washed once in 1× PBS. To prepare activated macrophages, the complete medium was supplemented with 10% horse serum (Gibco) and macrophages were activated with 100 U/ml recombinant mouse IFN-γ (Chemicon) and 50 ng/ml of tumor necrosis factor (TNF) for 48 h. Primary macrophages consistently represented 70 to 80% of the total cell population harvested, as determined by flow cytometry using a panmacrophage marker, anti-F4/80 antibody (eBioscience). A human THP-1 monocytoid cell line (ATCC TIB-202; ATCC, MD, USA) was maintained at 37°C and 5% CO_2 in HEPES buffered RPMI 1640 (Sigma-Aldrich, St. Louis, MO, USA) medium with 10% heat-inactivated fetal bovine serum (FBS), 2 mM L-glutamine, 10 mM HEPES, 1 mM sodium pyruvate, 4,500 mg/liter glucose, and 1,500 mg/liter sodium bicarbonate (pH 7). When needed, cells were expanded into 75-cm^2 flasks and were activated with retinoic acid (RA; 1 μM) and vitamin D_3 (VD; 1 μM) for 3 days as described previously (34). For survival assays, BMMO monolayers (5×10^4 cells/well) or RAVD-activated THP-1 cells (2.5×10^4 cells/well) in 24-well tissue culture plates (Nunc) were incubated with mycobacteria at multiplicities of infection (MOI) of 2 and 5, respectively, for 45 min in their respective incomplete culture media (culture media without penicillin-streptomycin and FBS). Infected cells were washed twice with 1× PBS, and the respective complete culture medium without penicillin-streptomycin was

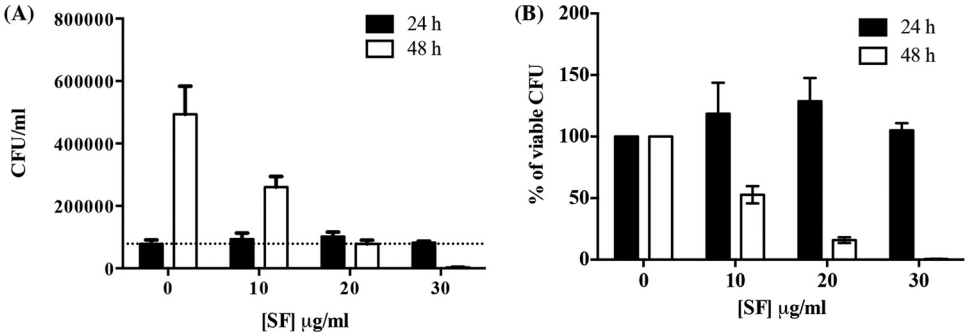

FIG 1 Mycobactericidal activity of a lysosomal soluble fraction (SF) prepared from activated primary murine macrophages. Mid-log-phase *in vitro* cultures of *M. tuberculosis* CDC1551 strain were coincubated for 24 or 48 h with a lysosomal SF prepared from activated primary murine macrophages at the indicated concentrations or with SF buffer only. (A) The treated bacteria were then plated on 7H11 agar and enumerated for viable CFU after 16 days of incubation at 37°C. The dotted line represents the initial inoculum. (B) Results are expressed as a percentage of viable CFU obtained with buffer only at their respective times of incubation. Data shown are the means ± standard deviations (SD) from triplicates.

added to each well. At the indicated time points, cells were washed with 1× PBS and lysed with 0.1% Triton X-100 (Sigma-Aldrich) to release the intracellular bacteria. The cell lysates were serially diluted in 7H9 medium and plated on 7H11 agar. The number of CFU was enumerated after incubation at 37°C for 16 days.

Statistical analysis. Statistical significance was assessed by the Student *t* test, and two-tailed *P* values of less than 0.05 were considered statistically significant.

Accession number. The data discussed in this publication have been deposited in NCBI's Gene Expression Omnibus (GEO) and are accessible through GEO series accession number GSE68337.

RESULTS AND DISCUSSION

The LivE model. The lysosomal *in vitro* exposure (LivE) model consists of the direct exposure of *M. tuberculosis* to the soluble fraction of lysosomes (SF) purified from activated murine bone marrow-derived macrophages (BMMO) based on a previously described protocol (27). The mycobactericidal activity of SF preparations was determined by incubating mid-log-phase *M. tuberculosis* cultures with a range of SF total protein concentrations for 24 and 48 h. As previously reported (27), the mycobactericidal activity of SF was found to be both time and concentration dependent (Fig. 1A). *M. tuberculosis* remained viable and unaffected in its growth rate after 24 h of incubation within the range of SF concentrations tested, as evidenced by CFU values being comparable to those of the positive control (buffer only) at 24 h. In contrast, a significant and dose-dependent reduction in viable CFU was observed after 48 h of coincubation.

Based on the growth profiles observed, we defined the following LivE conditions, ranging from noninhibitory to cidal upon SF exposure. Noninhibitory conditions consist of exposing *M. tuberculosis* to 10 to 30 μg/ml SF for 24 h, which led to growth comparable to 24 h of incubation with buffer only (24 h control) (Fig. 1). The subinhibitory condition was achieved by exposing *M. tuberculosis* to 10 μg/ml SF for 48 h and was characterized by a significant decrease in cell viability compared to the 48-h buffer control (Fig. 1) but a greater number of viable CFU compared to the 24-h control (Fig. 1A). The inhibitory condition was obtained upon incubation of *M. tuberculosis* in the presence of 20 μg/ml SF for 48 h, which resulted in a concentration of viable bacteria that was comparable to the inoculum concentration and significantly lower than that obtained with the 48-h untreated control (Fig. 1A and B). This suggested that incubation with 20 μg/ml SF for 48 h led to an apparent replication arrest, which can be the result of (i) a true arrest in replication where mycobacteria cease dividing but do not die, as described for other stress conditions, such as hypoxia (35) or starvation (36), or (ii) equal killing and replication rates that cancel each other out. Finally, the cidal condition was observed when *M. tuberculosis* was incubated with 30 μg/ml SF for 48 h, which resulted in a drastic reduction in viable CFU compared to the 48-h control (Fig. 1B).

RNA sequencing of *M. tuberculosis* in the LivE model. To investigate the transcriptome profile of *M. tuberculosis* upon exposure to SF, *M. tuberculosis* was exposed to noninhibitory (10 μg/ml SF, 24 h), subinhibitory (10 μg/ml SF, 48 h), and inhibitory (20 μg/ml SF, 48 h) conditions, with buffer only (0 μg/ml SF 24 h and 48 h) as the reference control. Illumina sequencing was performed on biological triplicates of cDNA libraries prepared from mRNA extracted from the SF-treated *M. tuberculosis* cultures. High-quality paired-end sequence reads were generated for each sample and were aligned with the *M. tuberculosis* CDC1551 parental reference genome, revealing coverage of more than 264 for all samples and indicating a high accuracy in the sequences generated. More than 89% of the sequence tags were mapped to the annotated CDS in the sense orientation. Differential expression analysis was performed with the R edgeR package (see Materials and Methods). We observed that the number of differentially expressed *M. tuberculosis* genes increased with increasing growth-inhibitory SF conditions, with more genes being induced than repressed, as illustrated in the volcano plots (Fig. 2). In addition, the majority of the genes found to be modulated under noninhibitory conditions were further modulated under the subinhibitory and inhibitory conditions.

The inhibitory LivE condition (iLivE) of 20 μg/ml for 48 h was then selected for further analysis, where the apparent replication appears to resemble the nonreplicative state described for mycobacteria exposed to other environmental stresses, such as hypoxia (35) or nutrient starvation (36) (Fig. 1). The iLivE *M. tuberculosis* genes were short-listed based on an FDR of <0.01 and disregarding genes with expression read counts of <5 (see Table S1 in the supplemental material). Gene function annotation was performed using DAVID and TBDB databases. The distribution of iLivE *M. tuberculosis* genes into different functional categories showed that a significant number of genes were involved in cell wall remodeling and substrate transport, intermediary metabolism and respira-

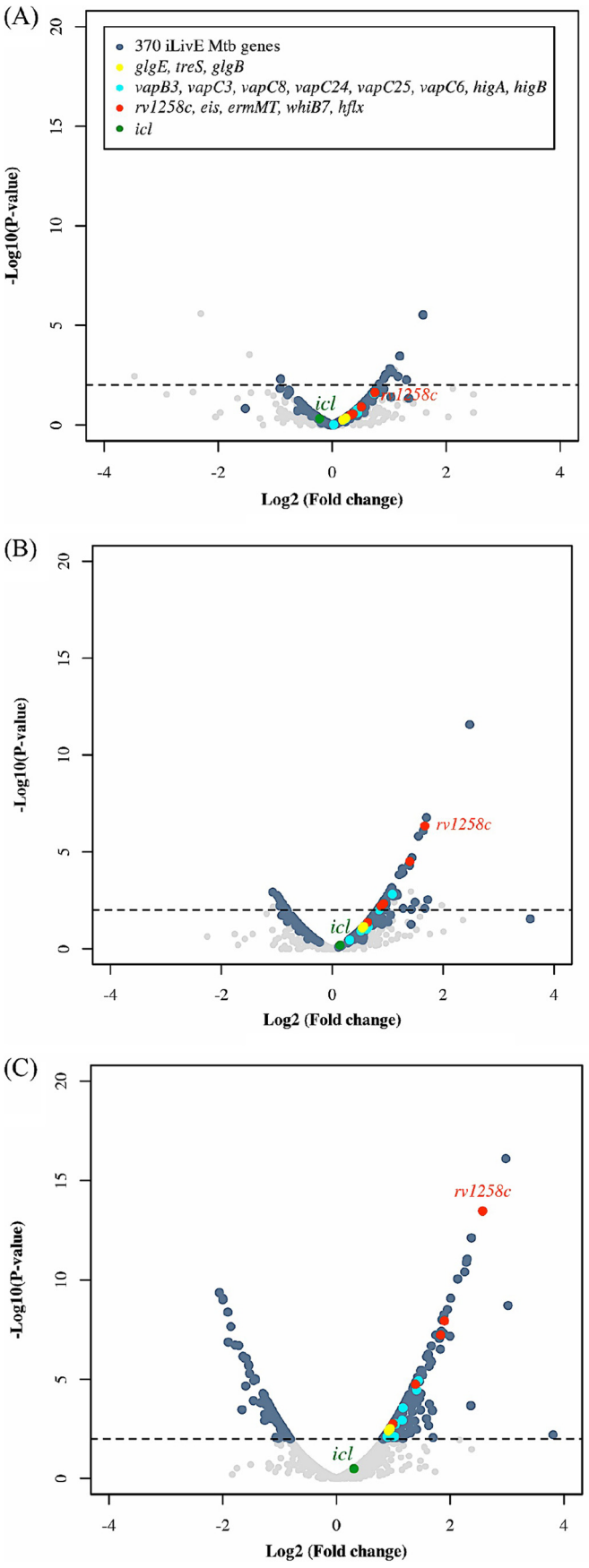

TABLE 1 Functional categories representing the iLivE *M. tuberculosis* transcriptome

Functional category[a]	No. of genes[b]	
	Induced	Repressed
Cell wall and cell processes	27	15
Information pathways	17	2
Insertion sequences and phages	10	
Intermediary metabolism and respiration	41	20
Metabolism	13	13
PE/PPE	5	7
Pseudogenes[c]	8	
Regulatory proteins	15	2
Virulence, detoxification, and adaptation	29	11
Unknown	8	5
Conserved hypotheticals	91	31
Total	264	106

[a] Functional annotations were obtained from TB Database (http://www.tbdb.org).
[b] The number of induced and repressed genes is given for each gene category.
[c] Genes that are not annotated in the *M. tuberculosis* H37Rv background.

tion, lipid metabolism, information pathways, regulatory proteins, and virulence, detoxification, and adaptation (Table 1). In total, there were 264 upregulated (Table 2) and 106 downregulated (Table 3) iLivE *M. tuberculosis* genes.

Validation of RNA-seq data. To validate the gene expression changes observed by RNA-seq analysis of the iLivE *M. tuberculosis* transcriptome, we selected a number of genes that were either highly modulated or of functional relevance and performed qRT-PCR on *M. tuberculosis* exposed to the same iLivE conditions (20 μg/ml for 48 h). The *icl* gene was used as a negative control, given its nonsignificant regulation under iLivE (fold change, 1.24; *P* value of 0.16). A comparable trend in fold changes obtained with both qRT-PCR and RNA-seq was observed for all selected genes (Fig. 3), thereby validating the iLivE *M. tuberculosis* transcriptome profile generated by RNA sequencing.

iLivE *M. tuberculosis* expresses a unique transcriptome. (i) General stress responses. The hostile nature of the lysosomal content undoubtedly imposes stress on *M. tuberculosis*. Under iLivE conditions, we observed the induction of several markers of general stress response, which includes a number of chaperone protein-encoding genes (*groEL1*, *groEL2*, *groES*, *grpE*, *dnaJ1*, *dnaK*, and *hspR*) that are involved in the folding and translocation of polypeptides and DNA repair (*dinF* and *dinX*) (37) (Table 2). These genes have also been reported to be upregulated during BMMO infections (10, 11, 30) and in lungs from TB patients (38), indicative of a stressful environment during infection partly contributed by the lysosomal contents. Furthermore, upregulation of the Clp proteases, particularly *clpP1*, *clpP2*, and *clpC2*, suggests prevalent protein degradation in iLivE *M. tuberculosis*. This observation may indicate a homeostatic response to prevent toxic accumulation of misfolded and aggregated proteins generated under stressed conditions (39). ClpP1 and ClpP2 have been reported

FIG 2 Volcano plots of *M. tuberculosis* genes in the LivE model. Transcriptomes of *M. tuberculosis* exhibited differential expression under noninhibitory (10 μg/ml SF, 24 h) (A), subinhibitory (10 μg/ml SF, 48 h) (B), and inhibitory (20 μg/ml SF, 48 h) (C) conditions. A total of 4,293 *M. tuberculosis* CDC1551 genes were annotated.

TABLE 2 Genes induced in iLivE *M. tuberculosis*

Functional category[a]	Designation for strain: CDC1551[b]	H37Rv	Gene	Description	Fold change	SD
Cell wall and cell processes	MT0201	Rv0191		Sugar transporter family protein	1.93	0.2
	MT0409	Rv0399c	*lpqK*	Putative lipoprotein	2.37	0.5
	MT0623	Rv0593	*mce2E* (*lprL*)	Mce family protein	1.81	0.2
	MT0700	Rv0671	*lpqP*	Lipoprotein	2.09	0.3
	MT0961	Rv0934	*pstS1* (*phoS1*)	Periplasmic phosphate-binding lipoprotein	1.90	0.8
	MT1013	Rv0985c	*mscL*	Large-conductance ion mechanosensitive channel	1.95	0.2
	MT1297	Rv1258c	*tap*	Putative Tap-like membrane efflux pump	5.94	0.3
	MT1503	Rv1456c		Antibiotic transport membrane ABC transporter	1.82	0.5
	MT1519	Rv1473		Probable macrolide transport ATP-binding protein ABC transporter	1.89	0.4
	MT1642	Rv1607	*chaA*	Cation/proton antiporter	1.97	0.3
	MT1926	Rv1877		Drug transporter	1.94	0.4
	MT1973	Rv1922		Peptidase, putative	1.88	0.8
	MT1997	Rv1946c	*lppG*	Possible lipoprotein	1.84	0.9
	MT2016	Rv1964	*yrbE3A*	Membrane protein	2.05	1.3
	MT2031	Rv1979c		Amino acid permease	2.03	0.5
	MT2040	Rv1986		Putative amino acid transporter	2.08	0.9
	MT2097	Rv2037c		Conserved transmembrane protein	1.84	0.5
	MT2100	Rv2040c		Sugar ABC transporter, permease protein	1.87	0.7
	MT2101	Rv2041c		Sugar ABC transporter, sugar-binding protein	1.83	1.2
	MT2334	Rv2273		Probable conserved transmembrane protein	2.00	1.2
	MT2339	Rv2281	*pitB*	Putative phosphate permease	3.59	1.5
	MT2469	Rv2398c	*cysW*	Sulfate transport membrane protein ABC transporter	1.93	0.6
	MT2471	Rv2400c	*sbp*	Sulfate ABC transporter substrate-binding protein	1.85	0.4
	MT2598	Rv2522c		Peptidase, M20/M25/M40 family	1.80	0.2
	MT2901	Rv2835c	*ugpA*	Probable Sn-glycerol-3-phosphate transport integral membrane protein ABC transporter	2.22	0.8
	MT3080	Rv3000		Possible conserved transmembrane protein	3.11	1.4
	MT3951	Rv3843c		Probable conserved transmembrane protein	1.87	0.4
Information pathways	MT0691	Rv0662c		DNA-binding protein, CopG family, transcriptional repressor	2.08	1.0
	MT0699	Rv0670	*end*	AP endonuclease, family 2	2.01	0.5
	MT1338	Rv1299	*prfA*	Peptide chain release factor 1	2.01	0.3
	MT1463	Rv1420		Probable excinuclease ABC (subunit C nuclease)	1.77	0.3
	MT1589	Rv1537	*dinX*	DNA polymerase IV DinX	2.09	0.5
	MT2042	Rv1988	*ermMT*	rRNA adenine N-6-methyltransferase, putative	2.62	0.4
	MT2247	Rv2191		DNA polymerase III, epsilon subunit, putative	1.90	0.4
	MT2488	Rv2415c		*comE* operon protein 1, putative	2.50	0.7
	MT2535	Rv2460c	*clpP2*	ATP-dependent Clp protease proteolytic subunit 2	2.12	0.5
	MT2536	Rv2461c	*clpP1*	Probable ATP-dependent CLP protease proteolytic subunit 1	2.18	0.8
	MT2741	Rv2667	*clpC2*	ATP-dependent protease ATP-binding subunit	2.10	0.8
	MT2902	Rv2836c	*dinF*	DNA damage-inducible protein F, putative	1.92	0.6
	MT2904	Rv2838c	*rbfA*	Ribosome-binding factor A	2.02	0.5
	MT2905	Rv2839c	*infB*	Translation initiation factor IF-2	2.01	0.6
	MT2942	Rv2874	*dipZ*	Cytochrome *c* biogenesis protein	2.19	0.5
	MT3686	Rv3580c	*cysS*	Cysteinyl-tRNA synthetase 1	2.62	0.2
	MT3942	Rv3834c		SERYL-tRNA synthetase	1.84	0.4
Insertion sequences and phages	MT0850	Rv0829		IS*1605′*, transposase, truncation	2.08	2.4
	MT0873	Rv0850		IS*1606′*, transposase	2.02	1.2
	MT0948	Rv0921		IS*1535*, resolvase	2.13	1.0
	MT2069	Rv2013		IS*1607*, transposase	2.67	0.8
	MT2070	Rv2014		IS*1607*, transposase	2.11	0.2
	MT2497	Rv2424c		IS*1558*, transposase	2.48	1.1
	MT2732	Rv2655c		Possible PhiRv2 prophage protein	2.03	0.1
	MT2735	Rv2646		Integrase	1.94	1.0
	MT2953	Rv2885c		IS*1539*, transposase	1.80	0.7
	MT3573.3			Bacteriophage protein	1.85	0.2
Intermediary metabolism and respiration	MT0098	Rv0089		Putative methyltransferase	3.50	1.4
	MT0207	Rv0197	*lpqS*	Molybdopterin oxidoreductase	1.80	0.7
	MT0337	Rv0322	*udgA*	UDP-glucose 6-dehydrogenase	1.91	0.7
	MT0511	Rv0492c		Oxidoreductase, GMC family	1.94	0.3

(Continued on following page)

TABLE 2 (Continued)

Functional category[a]	Designation for strain: CDC1551[b]	H37Rv	Gene	Description	Fold change	SD
	MT0560	Rv0536	*galE3*	NAD-dependent epimerase/dehydratase family protein	1.80	0.4
	MT0777	Rv0753c	*mmsA*	Methylmalonate-semialdehyde dehydrogenase	2.24	1.2
	MT0888	Rv0865	*mog*	Probable molybdopterin biosynthesis protein	1.81	0.1
	MT0916	Rv0892		Monooxygenase, flavin-binding family	1.84	0.6
	MT1128	Rv1096		Polysaccharide deacetylase, putative	1.83	0.3
	MT1295	Rv1256c	*cyp130*	Probable cytochrome P450	1.79	0.5
	MT1339	Rv1300	*papM* (*hemK*)	N-methylase	1.91	0.3
	MT1368	Rv1326c	*glgB*	1,4-α-Glucan branching enzyme	1.89	0.5
	MT1369	Rv1327c	*glgE*	Glucanase	1.88	0.4
	MT1424	Rv1380	*pyrB*	Probable aspartate carbamoyltransferase	1.82	0.6
	MT1511	Rv1464	*csd*	Cysteine desulfurase	1.89	0.4
	MT1512	Rv1465		Nitrogen fixation protein NifU-related protein	1.77	0.3
	MT1636	Rv1600	*hisC1*	Probable histidinol-phosphate aminotransferase	1.77	0.3
	MT1658	Rv1622c	*cydB*	Membrane cytochrome D ubiquinol oxidase subunit II	1.85	0.3
	MT1659	Rv1623c	*cydA*	Membrane cytochrome D ubiquinol oxidase subunit I	1.98	0.3
	MT1667	Rv1631	*coaE*	Probable dephospho-CoA kinase	1.80	0.5
	MT1690	Rv1652	*argC*	Probable N-acetyl-gamma-glutamyl-phosphate reductase	1.80	0.9
	MT1767	Rv1726		Oxidoreductase, FAD binding	1.91	0.7
	MT1902	Rv1854c	*ndh-2*	NADH dehydrogenase	1.76	0.6
	MT1987	Rv1937		Ferredoxin reductase, electron transfer component, putative	1.78	0.7
	MT2103	Rv2043c	*pncA*	Pyrazinamidase/nicotinamidas	1.90	0.5
	MT2274	Rv2217	*lipB*	Lipoate biosynthesis protein B	1.91	0.7
	MT2336	Rv2276	*cyp121*	P450 heme-thiolate protein	2.25	1.0
	MT2511	Rv2436	*rbsK*	Ribokinase	1.84	0.9
	MT2572	Rv2497c	*bkdA* (*pdhA*)	Probable branched-chain keto acid dehydrogenase E1 component, alpha subunit	1.78	0.4
	MT2797	Rv2725c	*hflX*	GTP-binding protein	1.99	0.3
	MT2965	Rv2897c		Mg chelatase	4.77	0.7
	MT2967	Rv2899c	*fdhD*	Formate dehydrogenase accessory protein	1.99	0.4
	MT2968	Rv2900c	*fdhF*	Possible formate dehydrogenase H	2.09	0.2
	MT3065	Rv2987c	*leuD*	3-Isopropylmalate dehydratase small subunit	1.86	0.2
	MT3066	Rv2988c	*leuC*	3-Isopropylmalate dehydratase large subunit	2.10	0.4
	MT3224	Rv3137		Inositol monophosphatase family protein	1.95	0.7
	MT3283	Rv3192		Putative luciferase	2.52	1.2
	MT3514	Rv3406		Putative dioxygenase	2.46	0.7
	MT3687	Rv3581c	*ispF*	Probable 2C-methyl-d-erythritol 2,4-cyclodiphosphate synthase	1.82	0.2
	MT3813	Rv3710	*leuA*	2-Isopropylmalate synthase	1.77	0.4
	MT3950	Rv3842c	*glpQ1*	Glycerophosphoryl diester phosphodiesterase	2.43	0.5
Metabolism	MT0590	Rv0564c	*gpsA* (*gpdA1*)	Probable glycerol-3-phosphate dehydrogenase	2.06	0.2
	MT0776	Rv0752c	*fadE9*	Acyl-CoA dehydrogenase	2.43	1.1
	MT1162	Rv1130	*prpD*	Possible methylcitrate dehydratase	3.62	0.3
	MT1163	Rv1131	*gltA1* (*prpC*)	Probable methylcitrate synthase	3.70	0.3
	MT1518	Rv1472	*echA12*	Possible enoyl-CoA hydratase	1.80	0.6
	MT1983	Rv1933c	*fadE18*	Acyl-CoA dehydrogenase, putative	1.91	0.4
	MT1984	Rv1934c	*fadE17*	Acyl-CoA dehydrogenase	3.09	1.5
	MT2243	Rv2188c	*pimB*	Mannosyltransferase	1.96	0.2
	MT2599	Rv2523c	*acpS*	Holo-[acyl-carrier protein] synthase	1.90	0.3
	MT2730	Rv2953		Enoyl reductase, may be involved in phenolpthiocerol and phthiocerol dimycocerosate (dim) biosynthesis	2.18	1.4
	MT3081	Rv3001c	*ilvC*	Ketol-acid reductoisomerase	1.98	0.3
	MT3082	Rv3002c	*ilvH* (*ilvN*)	Acetolactate synthase, small unit	2.31	0.4
	MT3083	Rv3003c	*ilvB*	Acetolactate synthase, large unit	2.37	0.5
PE/PPE	MT0369	Rv0354c	*ppe7*	PPE family protein	1.86	0.4
	MT0778	Rv0754		PE_PGRS11	2.41	0.6
	MT2505	Rv2430c	*ppe41*	PPE41	1.77	0.9
	MT3637	Rv3533c		PPE62	2.10	0.0
	MT3701	Rv3595c	*pe_pgrs59*	PE/PGRS protein	1.85	0.2
Regulatory proteins	MT0222	Rv0212c	*nadR*	AsnC family transcriptional regulator	4.02	0.6
	MT0368	Rv0353	*hspR*	Probable heat shock protein transcriptional repressor	2.22	0.5
	MT0481	Rv0465c		Transcriptional regulator	2.24	0.9

(Continued on following page)

TABLE 2 (Continued)

Functional category[a]	Designation for strain: CDC1551[b]	H37Rv	Gene	Description	Fold change	SD
	MT0514	Rv0494		Transcriptional regulator, GntR family	1.97	0.1
	MT0605	Rv0576		Transcriptional regulator, ArsR family	2.57	0.1
	MT0849	Rv0827	*kmtR*	Transcriptional regulator, ArsR family	1.93	0.7
	MT1161	Rv1129c		Probable transcriptional regulator protein	4.38	0.8
	MT1440	Rv1395		Transcriptional regulator, AraC family	1.86	0.1
	MT1520	Rv1473A		Possible transcriptional regulatory protein	2.22	1.1
	MT1960	Rv1909c	*furA*	Ferric uptake regulation protein	3.86	1.3
	MT2039	Rv1985c		Transcription regulator	2.60	0.1
	MT2073	Rv2017		Transcriptional regulatory protein	2.75	1.9
	MT2386	Rv2324		Transcriptional regulator, AsnC family	1.89	1.1
	MT2980	Rv2912c		Probable transcriptional regulatory protein, TetR family	2.19	0.4
	MT3290.1	Rv3197A	*whiB7*	Probable transcriptional regulatory protein, WhiB-like	3.56	0.6
Virulence, detoxification and adaptation	MT0134	Rv0126	*treS*	Trehalose synthase, alpha-amylase family protein	1.92	0.4
	MT0254	Rv0240	*vapC24*	Possible toxin	2.04	0.5
	MT0265	Rv0251c	*hsp*	Heat shock protein, HSP20 family	3.06	2.4
	MT0289	Rv0277c	*vapC25*	Possible toxin	2.25	0.6
	MT0365	Rv0350	*dnaK*	Probable chaperone protein	3.00	1.0
	MT0366	Rv0351	*grpE*	Probable GrpE protein	3.36	1.5
	MT0367	Rv0352	*dnaJ1*	Chaperone protein	2.70	1.0
	MT0397	Rv0384c	*clpB*	Endopeptidase ATP binding protein chain B, heat shock protein F84.1	1.77	0.4
	MT0456	Rv0440	*groEL2*	60-kDa chaperonin 2	2.78	1.3
	MT0574	Rv0549c	*vapC3*	Possible toxin	1.85	0.6
	MT0575	Rv0550c	*vapB3*	Possible antitoxin	2.23	0.6
	MT0618	Rv0589	*mce2A*	Mce family protein	1.76	0.2
	MT0621	Rv0591	*mce2C*	Mce family protein	2.56	0.1
	MT0685	Rv0656c	*vapC6*	Possible toxin	2.65	0.3
	MT0693	Rv0665	*vapC8*	Possible toxin	2.02	2.7
	MT1296	Rv1257c		Probable oxidoreductase	2.27	0.2
	MT1959	Rv1908c	*katG*	Catalase-peroxidase	2.34	0.2
	MT1961	Rv1910c		Hypothetical exported protein	2.09	0.1
	MT2004	Rv1955	*higB*	Possible toxin	2.72	0.9
	MT2005	Rv1956	*higA*	Possible antitoxin	2.05	0.6
	MT2018	Rv1966	*mce3A*	Mce family protein	2.05	0.4
	MT2489	Rv2416c	*eis*	Enhanced intracellular survival protein	3.73	0.6
	MT2503	Rv2428	*ahpC*	Alkyl hydroperoxide reductase C protein	2.19	0.6
	MT2504	Rv2429	*ahpD*	Alkyl hydroperoxide reductase D protein	2.22	1.1
	MT2941	NA		Prevent-host-death family protein	3.00	3.8
	MT3526	Rv3417c	*groEL1*	60-kDa chaperonin 1	3.18	2.3
	MT3527	Rv3418c	*groES*	10-kDa chaperonin	2.79	1.6
	MT3771	Rv3670	*ephE*	Epoxide hydrolase	2.11	0.8
	MT3949**	Rv3841	*bfrB*	Bacterioferritin	2.21	0.7

[a] Conserved hypothetical, unknown, and pseudogenes are listed in Table S1 in the supplemental material.
[b] **, DosR-dependent genes.

previously to play an important role in *M. tuberculosis* pathogenesis and represent potential drug targets (40). More recently, ClpP1 has been used in a novel target mechanism-based whole-cell screening assay and was used to successfully identify bortezomib as a new lead compound for tuberculosis therapy (41).

(ii) Metabolic reprogramming. Metabolic adaptations to host fatty acids and cholesterol by intracellular *M. tuberculosis* have been reported in transcriptomics studies from macrophage and mouse infections (11, 13, 15, 30, 42). Upregulation of *prpC* and *prpD* was observed in iLivE *M. tuberculosis* (Table 2). These genes encode key enzymes of the methylcitrate cycle and help *M. tuberculosis* detoxify propionyl-coenzyme A (CoA), a product from fatty acid catabolism during intracellular survival (43). However, induction of isocitrate lyase (*icl*) was not observed in iLivE *M. tuberculosis* (Fig. 2C), a key bifunctional enzyme that is induced simultaneously with *prpC* and *prpD* in intracellular *M. tuberculosis* (30) to utilize fatty acids via the glyoxylate shunt and methylcitrate cycle (44). The sole induction of *icl* has been reported in the presence of palmitic acid (11), suggesting that *icl* expression is directly modulated by the presence of fatty acids, which may explain its lack of induction in the fatty acid-free iLivE model. Reinforcing the notion that fatty acids are the preferred carbon source of intracellular *M. tuberculosis*, we also found a number of iLivE *M. tuberculosis* genes predicted with enzymatic functions involved in biochemical activation and β-oxidation of fatty acids. These include acyl-CoA dehydrogenase (*fadE9*, *fadE15*, *fadE17*, and *fadE18*), fatty acid-CoA ligase (*fadD5* and *fadD9*), enoyl-CoA hydratase (*echA12*), and lipases (*lipF* and *lipQ*) (Table 2). Most of

TABLE 3 Genes repressed in iLivE *M. tuberculosis*

Functional category[a]	Designation in strain: CDC1551[b]	H37Rv	Gene	Description	Fold change	SD
Cell wall and cell processes	MT0046	Rv0040c	*mtc28*	Secreted proline-rich protein	0.53	0.3
	MT0182	Rv0173	*mce1E* (*lprK*)	Mce family protein	0.48	0.2
	MT0356	Rv0341	*iniB*	Isoniazid-inducible gene protein	0.47	0.2
	MT0911	Rv0888		Probable exported protein	0.54	0.1
	MT1235	Rv1197	*esxK*	ESAT-6-like protein	0.34	0.1
	MT1236	Rv1198	*esxL*	ESAT-6-like protein	0.42	0.1
	MT1729	Rv1690	*lprJ*	Probable lipoprotein	0.43	0.1
	MT1779	Rv1737c	*narK2*	Nitrite extrusion protein, MFS	0.32	0.1
	MT1932	Rv1884c	*rpfC*	Probable resuscitation-promoting factor	0.55	0.3
	MT2411	Rv2346c	*esxQ*	ESAT-6-like protein	0.55	0.2
	MT2412	Rv2347c	*esxP*	ESAT-6-like protein	0.53	0.2
	MT2420	Rv2346c	*esxO*	ESAT-6-like protein	0.47	0.2
	MT2458	Rv2389c	*rpfD*	Resuscitation-promoting factor	0.51	0.2
	MT3988	Rv3874	*esxB* (*cfp10*)	10-kDa ESAT-6-like protein	0.56	0.2
	MT3989	Rv3875	*esxA* (*esat-6*)	ESAT-6-like protein	0.52	0.2
Information pathways	MT2669	Rv2592c	*ruvB*	Holliday junction ATP-dependent DNA helicase	0.45	0.3
	MT3347	Rv3249c		Transcriptional regulator, TetR family	0.41	0.3
Intermediary metabolism and respiration	MT0037	Rv0032		Aminotransferase	0.47	0.1
	MT0266	Rv0252	*nirB*	Probable nitrite reductase [NAD(P)H], large subunit	0.54	0.2
	MT0738	Rv0711	*atsA*	Possible arylsulfatase	0.51	0.3
	MT1449	Rv1405c		Methyltransferase	0.43	0.2
	MT1603	Rv1552	*frdA*	Probable fumarate reductase	0.51	0.0
	MT1604	Rv1553	*frdB*	Fumarate reductase, iron-sulfur subunit	0.42	0.0
	MT1606	Rv1555	*frdD*	Fumarate reductase membrane anchor subunit	0.42	0.1
	MT1778**	Rv1736c	*narX*	Probable nitrate reductase	0.51	0.9
	MT1904	Rv1856c		Possible oxidoreductase	0.54	0.2
	MT2063**	Rv2007c	*fdxA*	Ferredoxin	0.47	0.6
	MT2088**	Rv2029c	*pfkB*	6-Phosphofructokinase	0.36	0.5
	MT2401	Rv2338c	*moeW*	Possible molybdopterin biosynthesis protein	0.53	0.2
	MT3194	Rv3111	*moaC*	Molybdenum cofactor biosynthesis protein C 2	0.34	0.2
	MT3423	Rv3322c		Possible methyltransferase	0.37	0.1
	MT3424	Rv3323c	*moaDE*	Molybdopterin cofactor biosynthesis protein D/E	0.37	0.2
	MT3426	NA	*moaB3*	Probable pterin-4-alpha-carbinolamine dehydratase	0.28	0.2
	MT3427	NA	*moaA3*	Molybdenum cofactor biosynthesis protein A 3	0.27	0.2
	MT3849	Rv3741c		Possible oxidoreductase	0.57	0.3
	MT3850	Rv3742c		Possible oxidoreductase	0.52	0.3
	MT3969	Rv3854c	*ethA*	Monooxygenase	0.53	0.3
Metabolism	MT0038	Rv0033	*acpA* (*acpP*)	Acyl carrier protein	0.48	0.3
	MT0175	Rv0166	*fadD5*	Probable fatty-acid-CoA ligase	0.55	0.1
	MT0258	Rv1467c	*fadE15*	Acyl-CoA dehydrogenase	0.45	0.2
	MT1702	Rv1662	*pks8*	Probable polyketide synthase	0.55	0.2
	MT2559	Rv2485c	*lipQ*	Carboxylesterase family protein	0.50	0.3
	MT2667	Rv2590	*fadD9*	Fatty acid-CoA ligase	0.50	0.3
	MT3216**	Rv3130c	*tgs1*	Triacylglycerol synthase	0.24	0.1
	MT3326	Rv3229c	*desA3*	Linoleoyl-CoA desaturase, putative	0.55	0.2
	MT3348	Rv3250c	*rubB*	Rubredoxin	0.41	0.3
	MT3349	Rv3251c	*rubA*	Rubredoxin	0.47	0.3
	MT3350	Rv3252c	*alkB*	Transmembrane alkane 1-monooxygenase	0.44	0.3
	MT3591	Rv3847c	*lipF*	Probable esterase/lipase	0.53	0.2
	MT3933	Rv3825c	*pks2*	Mycocerosic acid synthase	0.51	0.2
PE/PPE	MT1233	Rv1195	*pe13*	PE family protein PE13	0.29	0.1
	MT1234	Rv1196	*ppe18*	PPE family protein PPE18	0.33	0.0
	MT1745	Rv1705c	*ppe22*	PPE family protein PPE22	0.49	0.2
	MT1746	Rv1706c	*ppe23*	PPE family protein PPE23	0.47	0.1
	MT2166	Rv2107	*pe22*	PE family protein PE22	0.42	0.1

(Continued on following page)

TABLE 3 (Continued)

Functional category[a]	Designation in strain: CDC1551[b]	H37Rv	Gene	Description	Fold change	SD
	MT3427.1	Rv3347	*ppe55*	PPE family protein PPE55	0.27	0.2
	MT3854	Rv3746c	*pe34*	PE family protein	0.42	0.2
Regulatory proteins	MT3230	Rv3143		Probable response regulator	0.53	0.2
	MT3870	Rv3765c	*tcrX*	Probable two-component transcriptional regulatory protein	0.51	0.2
Virulence, detoxification, and adaptation	MT0052	Rv0046c		1-l-myo-inositol-1-phosphate synthase	0.49	0.3
	MT0176	Rv0167	*yrbE1A*	Conserved integral membrane protein	0.54	0.2
	MT0178	Rv0169	*mce1A*	Mce family protein	0.54	0.1
	MT0179	Rv0170	*mce1B*	Mce family protein	0.54	0.1
	MT0180	Rv0171	*mce1C*	Mce family protein	0.52	0.2
	MT0181	Rv0172	*mce1D*	Mce family protein	0.50	0.2
	MT0183	Rv0174	*mce1F*	Mce family protein	0.46	0.2
	MT2087	NA		Universal stress protein family protein	0.35	1.0
	MT2090**	Rv2031c	*hspX*	Alpha crystallin, 14-kDa antigen	0.25	0.0
	MT2698**	Rv2623	*TB31.7*	Universal stress protein family	0.43	0.5
	MT3598	Rv3494c	*mce4F*	Mce family protein	0.50	0.1

[a] Conserved hypothetical and unknown genes are listed in Table S1 in the supplemental material.
[b] **, DosR-dependent genes.

these genes have been reported previously to be modulated under various *in vitro* and *ex/in vivo* conditions (10, 11, 21, 24, 30) with the exception of *fadE17* and *fadE18*, which seem to be specifically upregulated in iLivE *M. tuberculosis*. Thus, it appears that the lysosomal content represents an environmental signal for the bacterium to upregulate genes involved in fatty acid beta-oxidation, perhaps in anticipation of the next round of infection upon lysis of the host cell.

(iii) Cell wall remodeling. With a lipid-rich cell wall envelope, mycobacterial cell wall remodeling is also tightly associated with its lipid metabolism (45) and can be a possible adaptive mechanism of *M. tuberculosis* when coping with a constantly changing host environment (46). In line with the apparent nonreplicative state of iLivE *M. tuberculosis*, we detected a downregulation of *pks2* and *desA3* (Table 3), which are essential genes for the biosynthesis of main cell wall components of mycobacteria (47). On the contrary, *pks2* expression was found to be induced upon phagosome acidification (12, 20), an environmental cue that is not represented in the LivE model, where pH is maintained at 6.8. Interestingly, *desA3* was previously proposed to be involved in regulating the membrane fluidity necessary for physiological function (48). Repressed expression of *desA3* in iLivE *M. tuberculosis* suggests reduced cell membrane fluidity, leading to limited barrier permeability that could limit drugs from gaining access to their bacterial targets and consequently conferring phenotypic drug resistance.

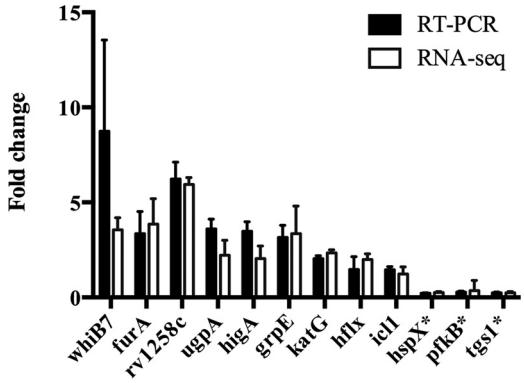

FIG 3 Validation by quantitative real-time PCR analysis of selected iLivE *M. tuberculosis* genes. Exponential *M. tuberculosis* culture was coincubated with SF under inhibitory conditions (20 μg/ml SF, 48 h) or with buffer only (control). Total RNA was extracted and real-time PCR was performed using specific primers listed in Table S7 in the supplemental material. For each gene, the average from technical triplicates was calculated and expressed as fold change compared to the gene expression level measured in the control. Fold changes (black bar) were compared to those obtained by RNA-seq (open bar). Data shown are the means ± standard deviations (SD) from triplicates. *, DosR-dependent genes.

Furthermore, consistent with observations in the short-term macrophage infection model (10, 11), the *mce1* operon (*yrbE1A* and *mce1A-F*) was downregulated in iLivE *M. tuberculosis* (Table 3). Deletion of this operon has been associated with (i) accumulation of free mycolic acids in the mycobacterial cell wall (49), (ii) a hypervirulent infection profile in mice with an impaired ability to trigger a proinflammatory response (50), and (iii) *in vitro* phenotypic drug tolerance (51). Therefore, *mce1* downregulation in iLivE *M. tuberculosis* may lead to changes in its cell wall mycolic acid composition, which could contribute to altered drug susceptibility of *M. tuberculosis*.

Finally, in iLivE *M. tuberculosis* we measured the upregulation of *pstS1*, which encodes a mycobacterial cell wall adhesin that has been demonstrated to promote phagocytosis of mycobacteria via binding to the mannose receptor (52). This implies an increased ability of bacilli to infect neighboring host cells when released from apoptotic macrophages.

Downregulation of *dosR*-dependent genes. Induction of the transcriptional factor DosR, involved in activation of the dormancy program in *M. tuberculosis* (53), has been associated with hypoxic conditions within TB granulomas (54) and reactive nitro-

gen intermediates produced by activated macrophages (55). The Dos regulon, which comprises ~49 genes regulated by the DosR-S/T two-component system, has been described to respond to a variety of signals and stresses, including low-oxygen tension, S-nitrosoglutathione (GSNO), ethanol, and carbon monoxide (56). As expected, *dosR* expression was minimally modulated in the iLivE model (fold change, −1.3; *P* value of 0.25), since this model does not incorporate any of the above-mentioned stimuli. However, and interestingly, we observed significant modulation of 17 *dosR*-dependent genes in iLivE *M. tuberculosis*, among which 15 were downregulated (Table 3). The majority of these repressed *dosR*-dependent genes were also found downregulated in the long-term BMMO infection model (at day 8) (Table 3), and this was attributed to the sudden loss of cue(s) driving the DosR response at the later stage during macrophage infection (30), where the bacterium presumably has transited to a persistent state. Consistent with this, transient and early induction of *dosR*-dependent genes during the first 4 to 8 h, followed by a gradual decline to baseline within 24 h, was also reported in a defined hypoxia model (22).

Thus, these observations suggest that the gene expression signature of iLivE *M. tuberculosis* partially overlaps that profiled at the late stage of macrophage infection, which further supports the idea that mycobacteria at this stage of infection are exposed to a lysosomal environment. The data also suggest that genes previously identified as part of the Dos regulon also are regulated independently of DosR.

ESAT-6 and PE-PPE family of proteins. Genes encoding a cluster of ESAT-6-like proteins (*esat-6*, *cfp10*, *esxQ*, *esxP*, *esxK*, and *esxQ*) were notably downregulated in iLivE *M. tuberculosis* (Table 3). Consistent with this, the expression of *esxQ*, *esxP*, *esxK*, and *esxQ* genes was also found downregulated in resting and activated macrophages (10). ESAT-6 and CFP-10 have been identified as both virulence factors and protective antigens (57, 58). In contrast, the PE/PPE genes that were modulated in iLivE *M. tuberculosis* exhibited various expression trends in previous transcriptomics studies of macrophage (10, 11), mouse (42) infection models, and under *in vitro* stresses (21, 24) (see Table S1 in the supplemental material). Our analysis singled out PPE41 based on its consistent induced profile observed in *M. tuberculosis* from infected BMMO (11) and human macrophages (13), mouse lungs (42), and iLivE *M. tuberculosis* (see Table S1). The PE25/PPE41 protein complex was shown to induce dendritic cell activation and drive Th2-biased immune responses (59), whereas Th1-biased immune responses have long been known to be protective against tuberculosis (60). Downregulation of ESAT-6-like proteins and upregulation of PPE41 in iLivE *M. tuberculosis* indicates that the lysosomal environment contributes to subversion of the host immune system by *M. tuberculosis* toward nonprotective immune responses.

Fighting oxidative stresses. Exposure to inhibitory SF conditions upregulated several *M. tuberculosis* genes (*furA*, *katG*, *ahpC*, and *ahpD*) (Table 2) that are known to be instrumental in combating oxidative stresses mediated by reactive oxygen species (ROS) and reactive nitrogen intermediates (RNI) (61–63), which are abundantly produced in an activated macrophage. While *furA* and *katG* have been reported to be upregulated under *in vitro* oxidative stresses (11), their regulation under nonoxidative conditions, such as nutrient starvation (24), gradual hypoxia (21), static growth (26), and iLivE conditions (see Table S1 in the supplemental material), suggests that these genes respond to multiple environmental stimuli. Alternatively, intrinsic ROS production by the mycobacterial cell itself could also be responsible for inducing these genes. This hypothesis is supported by the upregulation of *Rv1464* and *Rv1465* ORFs (Table 2) from the SUF operon that encodes the alternative mycobacterial iron-sulfur cluster machinery (64). Furthermore, high production of ROS was detected in nonreplicating nutrient-starved mycobacteria and was attributed to cytochrome P450 (CYP)-based metabolism of ketone bodies generated from triacylglycerol (TAG) stores during nutrient starvation (our unpublished observations). Coincidentally, *cyp121* and *cyp130* were found to be upregulated in iLivE *M. tuberculosis* (Table 2). Thus, intracellular production of ROS through CYP activity upon lysosomal exposure represents an interesting possibility which remains to be further investigated.

Respiratory status. The respiratory status of *M. tuberculosis* is dependent on the microenvironment it encounters, such as the oxygen tension and availability of various carbon and nitrogen sources to act as terminal electron acceptors (65). Induction of bd-type terminal oxidase-encoding genes (*cydA* and *cydB*) and genes involved in nitrate respiration (*narK2*) were detected in iLivE *M. tuberculosis* (Table 2). This is consistent with a transitional respiratory state previously described for intracellular *M. tuberculosis* upon NO production following immune cell activation (65). In contrast, the fumarate reductase gene cluster *frdABD* was notably repressed in iLivE *M. tuberculosis*, which is consistent with the aerobic setup of the LivE model (Table 3). Induced expression of fumarate reductase was observed in activated BMMOs (11) in an NO-dependent manner and in hypoxic lung lesions from tuberculosis patients (38), and it was associated with anaerobic persistence (66). Interestingly, modulation of gene clusters encoding F_0F_1 ATP synthase (*atpA-H*) and NADH dehydrogenase 1 (*nuoA-N*), which are involved in aerobic respiration, was not observed in iLivE *M. tuberculosis*. Along with ribosomal proteins (*rps*), these regulons were also notably repressed during regulated slow growth (67) and in models of persistence where mycobacterial replication arrest is induced by reduced oxygen and/or nutrient availability (68, 69). As mentioned earlier, the true replicative/nonreplicative status of mycobacteria during SF exposure remains to be further characterized.

Meta-analysis with transcriptomes of intracellular *M. tuberculosis* from macrophage infection models. The experimental setup of the LivE model was designed to (partially) mimic exposure of *M. tuberculosis* to the lysosomal content upon phagosome/autophagosome maturation during macrophage infection. Thus, we subjected the iLivE *M. tuberculosis* transcriptome profile to a comparative analysis with selected key transcriptome profiling studies of intracellular *M. tuberculosis* during infection in BMMO and human macrophages (THP-1). With the caveat that each study used different infection conditions, different macrophage types, and different *M. tuberculosis* strains, our analysis revealed that 193 out of 370 iLivE genes overlapped genes from these macrophage infection studies, while 177 did not overlap any of the studies considered (Fig. 4; see also Tables S2 and S3 in the supplemental material). As expected, the largest overlap was observed with the BMMO infection models (168 out of 193) (Fig. 4; see also Table S3), suggesting a partial recapitulation of intramacrophage lysosomal exposure in the LivE model. However, it is believed that in some of these BMMO infection models, mycobacteria reside primarily in a phagosomal environment due to phagosome

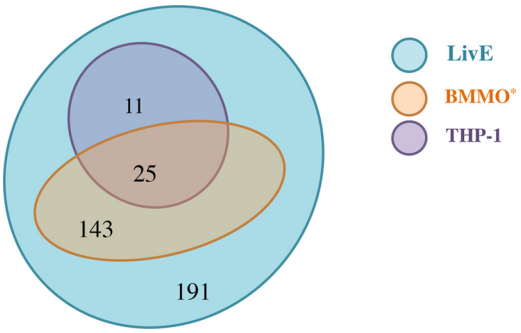

FIG 4 Venn diagram comparing transcriptional profiles of *M. tuberculosis* under iLivE conditions and during macrophage infections. THP-1, human macrophage model; iLivE, inhibitory condition of lysosomal *in vitro* exposure. The asterisk indicates that the gene is included if it is modulated in at least one of the three primary murine macrophage (BMMO) infection models.

maturation arrest. Therefore, it is possible that some of these overlapping genes are also modulated by stimuli present in the phagosome prior to lysosomal fusion. To further refine the lysosome-specific gene responses triggered under iLivE conditions, we excluded iLivE genes that were modulated during resting macrophage infection reported by Homolka et al. (10) and Schnappinger et al. (11), where mycobacteria are believed to reside mainly within phagosomes. Furthermore, since the process of infection is not synchronized, the bacilli retrieved from the infected macrophage population at each time point consist of a heterogeneous population of bacteria which have been exposed to various intracellular environments, ranging from early endosome to lysosomal compartment. Therefore, the mycobacterial transcriptional response measured is likely to be heterogeneous, reflecting the responses to various intracellular microenvironments. On the contrary, in the iLivE model, the mycobacterial transcriptional response is expected to be more homogeneous. Therefore, we postulated that fold changes measured in iLivE *M. tuberculosis* are likely to be greater in magnitude than those measured in activated macrophages. Thus, a more stringent cutoff value was arbitrarily implemented for each gene by either dividing (upregulation) or multiplying (downregulation) their expression fold change by 1.5, leading to selection of 41 iLivE *M. tuberculosis* genes (see Table S6). Among these 41 genes, most of the general stress response markers (*groEL1*, *groES*, and *dnaJ1*) were present, further supporting the increased level of stress experienced by bacilli exposed to the lysosomal environment. Interestingly, we found several antibiotic resistance-related genes, namely, *eis* (*Rv2416c*), *ermMT* (*Rv1988*), and *tap* (*Rv1258c*), with remarkably increased expression under iLivE conditions. Although the mechanisms by which they induce antibiotic resistance are different (70–73), expression of all of these genes is under the control of the transcriptional factor WhiB7 (70), one of the earliest and most highly induced transcriptional regulators in *M. tuberculosis* during BMMO infection (12), and in response to numerous stress conditions (70, 74, 75). Thus, these findings strongly support that the lysosomal content induces a WhiB7-mediated phenotypic drug resistance in *M. tuberculosis*.

In contrast, we observed a limited number of overlapping genes (36 out of 370) between THP-1 macrophage infection and the iLivE model (Fig. 4), which is likely attributable to inherent physiological differences between a human macrophage cell line and a primary mouse-derived macrophage (SF was prepared from activated BMMO). Nevertheless, genes involved in oxidative stresses (*ahpC* and *ahpD*) and fatty acid metabolism (*prpC* and *prpD*) were found in the 25 iLivE gene subset that were commonly regulated in both BMMO and THP-1 infection models (Fig. 4; see also Table S3 in the supplemental material), indicative of a comparable intramacrophage environment between human and mouse macrophages. From the subset of 11 iLivE genes that overlap THP-1 macrophages only (Fig. 4; see also Table S3), it is worth mentioning *rpfD*, the product of which has been implicated in resuscitating mycobacteria from dormancy (76).

Our meta-analysis also revealed a significant number of genes (177 iLivE *M. tuberculosis* genes) that did not overlap any of the macrophage infection models analyzed (see Table S2 in the supplemental material). These nonoverlapping genes could represent a subset of lysosome-inducible genes, which were previously not detected in macrophage models due to nonsynchronized infection conditions, where only a small percentage of mycobacteria harvested from the infected macrophages actually reside inside the lysosomal compartment at one time. Among these nonoverlapping genes, we found *glgE*, *glgB*, and *treS* to be significantly upregulated (see Table S2). These genes are involved in the α-1,4-glucan pathway implicated in detoxification of maltose-1-phosphate (M1P) to α-glucan (77). Interestingly, loss of *glgE*, which encodes a maltosyltransferase, was reported to impair the bacterium's replication ability in lungs and spleen from infected BALB/c mice (77). This defect was attributed to cell toxicity from the accumulation of the phosphosugar intermediate, thus revealing α-glucan synthesis as a potential target for antimicrobials (77). Upregulation of *glgE* in iLivE *M. tuberculosis* further indicates that targeting of GlgE and the α-glucan synthesis pathway represents a viable therapeutic approach to kill intraphagolysosomal mycobacteria.

Among the nonoverlapping iLivE gene subset, a number of mycobacterial toxin/antitoxin (TA) systems were also significantly induced. They include *vapB3*, *vapC3*, and *vapC8* of the VapBC systems, which represents the largest family of bacterial TA systems (78). In addition, the HigBA1 TA system and three more VapC toxin-encoding genes, *vapC24*, *vapC25*, and *vapC6*, were upregulated (Table 2). Upregulation of TA systems in response to adverse conditions has been described in other bacterial species (79). Typically, bacterial TA systems are made of a toxin protein and a more labile antagonistic antitoxin, which can be a protein or noncoding RNA (80). Some of the mycobacterial VapC toxins have been shown to exert a bacteriostatic effect on mycobacterial growth through their RNase activity (81). While nutrient-starved *M. tuberculosis* cells and drug-tolerant *M. tuberculosis* persisters have been shown to express distinct sets of TA systems (25, 68), the VapBC TA systems could be exploited to induce toxicity in intramacrophage bacilli.

Finally, genes encoding cell wall-associated proteins, comprising transporters and lipoproteins, represent another prominent group of significantly induced nonoverlapping iLivE genes (see Table S2 in the supplemental material). The transporters were mainly associated with drug efflux (*Rv0191*, *Rv1877*, and *Rv1456c*) and uptake of sulfate, amino acids, and sugars (*cysW*, *Rv1979c*, and *pitB*), while the lipoproteins exhibited a plethora of predicted functions, including peptidoglycan cross-linking and remodeling (*lpqK* and *Rv1922*), degradation processes (*Rv0671*), host cell adhesion and invasion (*Rv0593*), and as solute binding proteins of

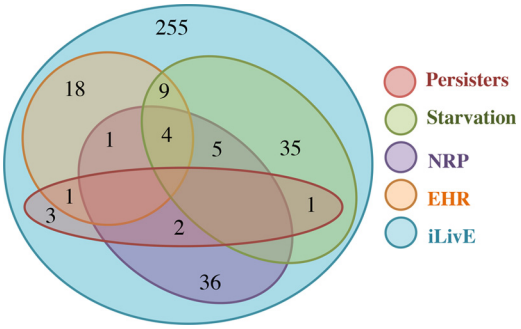

FIG 5 Venn diagram comparing transcriptional profiles of *M. tuberculosis* under iLivE conditions and various environmental stresses. EHR, defined hypoxic model; persisters, drug-tolerant persisters model; starvation, nutrient starvation model; NRP, gradual hypoxic model; iLivE, inhibitory condition of lysosomal *in vitro* exposure.

ABC transport systems (*sbp*) (82). This could represent responses to (i) membrane stresses induced by membrane-perturbing agents (antimicrobial cationic peptides present in the lysosomal SF), (ii) intracellular toxic accumulation arising from SF-induced metabolic changes, and/or (iii) membrane remodeling for nutrient-scavenging activities or to facilitate escape into the cytosol.

Meta-analysis with *M. tuberculosis* transcriptomes from *in vitro* stress models. Under *in vitro* conditions that are meant to reproduce some of the environmental cues encountered within a macrophage or a granuloma, exposure to gradual hypoxia (21), defined hypoxia (22), nutrient starvation (24), and antibiotics at incomplete sterilizing concentrations (25) induces *M. tuberculosis* persistence, characterized by nonreplication and phenotypic resistance to the TB drugs isoniazid and rifampin. The meta-analysis between iLivE *M. tuberculosis* transcriptome and *M. tuberculosis* transcriptomes profiled from these *in vitro* models indicates minimal overlap, which suggests that the physiological state of mycobacteria exposed to lysosomal SF significantly differs from that of hypoxic conditions, nutrient-starved conditions, or antibiotic-exposed mycobacteria (see Tables S4 and S5 in the supplemental material). Nevertheless, 115 iLivE genes overlapped at least one of these *in vitro* models of persistence, with only four genes (*echA12*, *hsp*, *higA*, and *Rv2036*) commonly regulated in all models considered, excluding the drug persisters model (Fig. 5; see also Table S5). The overlap between iLivE and at least one *in vitro* model here suggests that the same pathway is triggered by more than one environmental stimulus, as supported by a substantial number of regulatory proteins present in this gene subset (see Table S5), including multistress-induced transcriptional factor WhiB7. On the contrary, genes that are triggered by a specific environmental stimulus, such as acidic pH, induced *aprABC* locus (83), and hypoxia-driven *dosR*, were not found in the iLivE transcriptome due to the absence of these cues from the LivE model, highlighting a general limitation of *in vitro* models, where only one or a limited number of environmental stimuli are incorporated. On the other

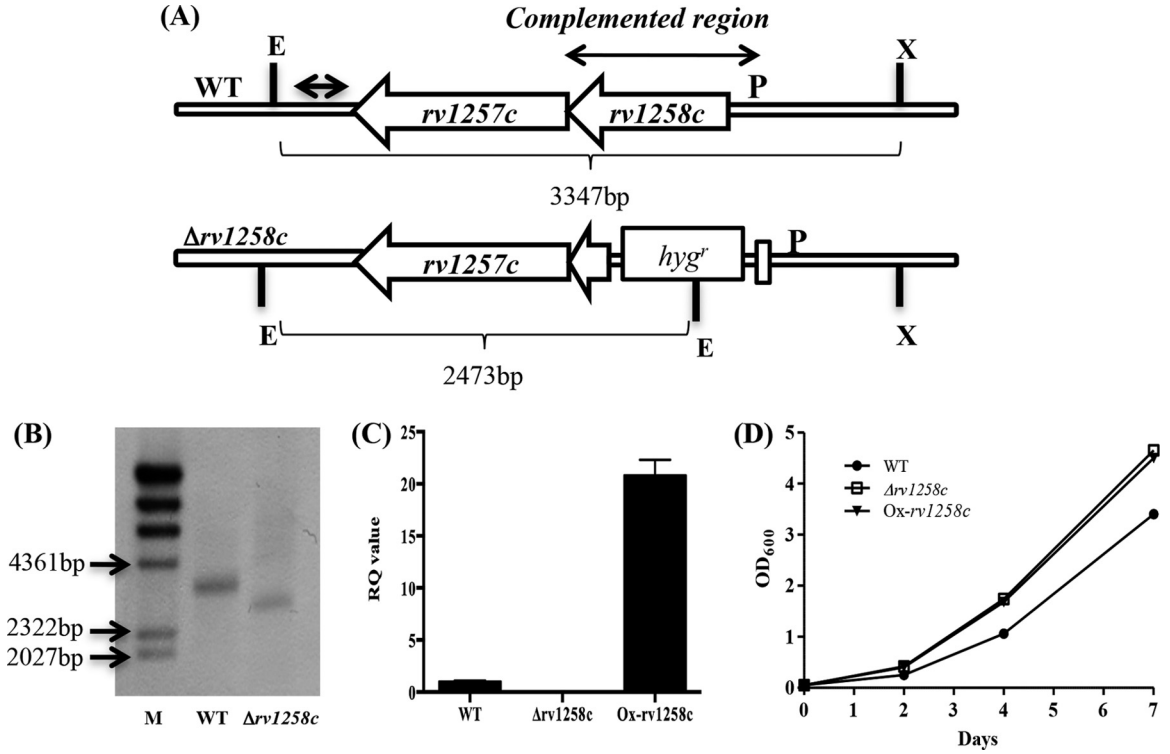

FIG 6 Construction of *M. tuberculosis* Δ*Rv1258c* mutant and its complemented strain, Ox-*Rv1258c*. (A) Schematic organization of CDC1551 *M. tuberculosis* *Rv1257c-1258c* locus in parental strain (WT). The mutant was obtained by introducing a *hyg* cassette into the *Rv1258c* ORF by double homologous recombination and complemented by reintegrating *Rv1258c* under the *M. tuberculosis hsp60* promoter (Ox-*Rv1258c*) into its genome. Southern blot probe and restriction enzyme sites are indicated (E, EcoRI; X, XmaI; probe, double-headed arrow). (B) Southern blot analysis. M, DIG-labeled molecular ladder. (C) Transcriptional activity of *Rv1258c* in WT, Δ*Rv1258c*, and Ox-*Rv1258c* strains as determined by real-time PCR analysis. Data are expressed as averages ± SD from triplicates. (D) *In vitro* growth kinetics of WT and Δ*rv1258c* strains and its complemented strain in 7H9 medium.

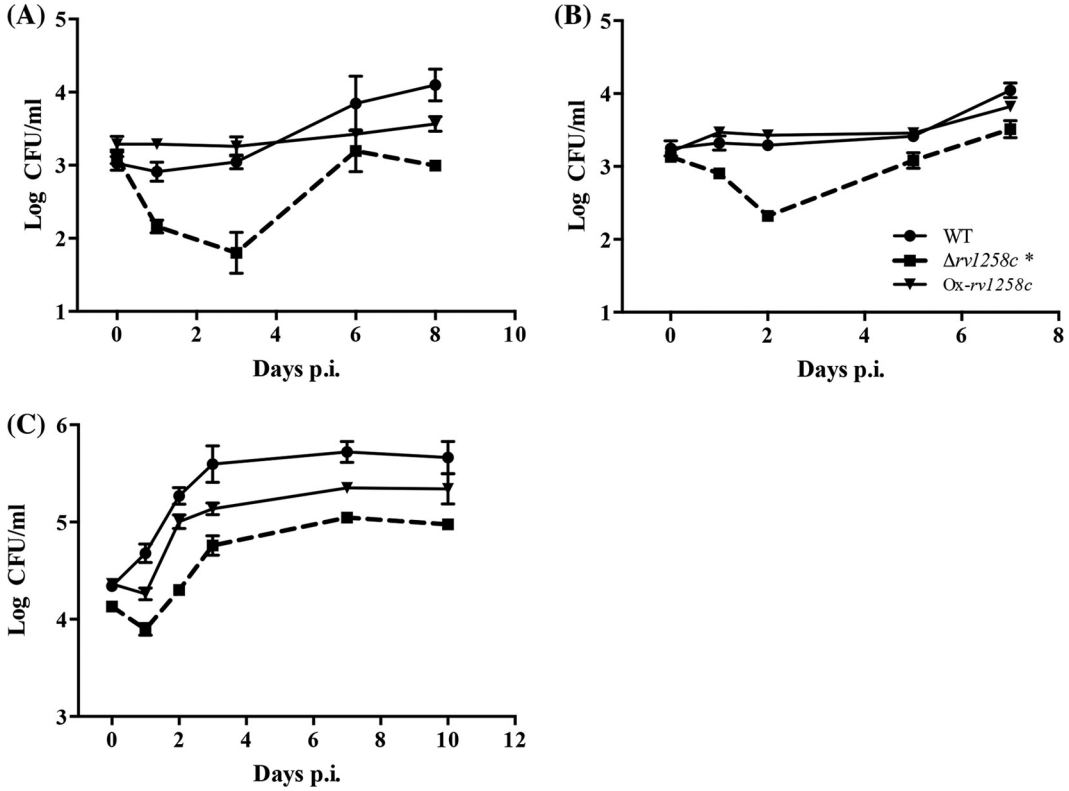

FIG 7 *M. tuberculosis* Δ*Rv1258c* strain survival profile in resting and activated macrophages. Resting (A) and activated (50 ng/ml of TNF and 100 U/ml of IFN-γ) (B) murine bone marrow-derived macrophages (BMMOs) were infected with *M. tuberculosis* strains at an MOI of 2. (C) Retinoic acid and vitamin D (RAVD)-activated THP-1 macrophages were infected at an MOI of 5. After 45 min of incubation, the infected cells were washed with PBS to remove extracellular bacteria (day 0 postinfection). At the indicated time points, the infected cells were lysed and viable CFU were recovered on 7H11 agar and enumerated. *, $P < 0.05$. Data shown are means ± SD from quadruplicates and are representative of two independent experiments.

hand, a large number (255) of iLiveE genes did not overlap any of the *in vitro* models considered in this meta-analysis and include genes involved in virulence detoxification pathways, cell wall processes, and intermediary metabolism (see Table S4). It is plausible that these genes are modulated by lysosome-specific stimuli that are not represented in the other *in vitro* models. The iLivE model therefore allows investigation of *M. tuberculosis* responses specific to a relevant and defined intramacrophage microenvironment, where the identification and biochemical characterization of host molecules with antimycobactericidal activity can be undertaken (27).

Validation of the LivE model. To support the relevance of our transcriptomics approach to study *M. tuberculosis* responses to the lysosomal environment, we selected one gene candidate, *Rv1258c*, which was found highly expressed under iLivE conditions and functionally relevant as a membrane Tap-like efflux pump (84–86). A previous study reported that *M. tuberculosis* transposon mutants of *Rv1258c* displayed reduced viability at 96 h postmacrophage infection (71). However, the authors did not confirm the observed attenuated phenotype by complementation study. Here, we constructed an *M. tuberculosis* Δ*Rv1258c* mutant by homologous recombination and its complemented strain, Ox-*Rv1258c*, by introducing the *Rv1258c* ORF under the expression of the constitutive *hsp60* promoter into the Δ*Rv1258c* mutant (Fig. 6A). Deletion of *Rv1258c* was confirmed by Southern blotting (Fig. 6B) and did not affect the transcription of the downstream gene *Rv1257c*, as assessed by real-time PCR (data not shown). Furthermore, qRT-PCR analysis showed that expression of *Rv1258c* was restored in the complemented strain Ox-*Rv1258c* with a 22-fold increase in transcriptional activity compared to the parental expression, likely due to the use of the strong mycobacterial *hsp60* promoter (Fig. 6C). The *in vitro* fitness of both the mutant and complemented strains was similar to that of the parental strain (Fig. 6D).

To confirm the role of *Rv1258c* during macrophage infection that was previously reported (71), resting and activated (100 U/ml IFN-γ and 50 ng/ml TNF) BMMOs were infected with WT, Δ*Rv1258c*, and complemented strains. A marked reduction in bacterial load of approximately one log was observed with the Δ*Rv1258c* mutant compared to the WT at 2 to 3 days postinfection in both resting and activated BMMOs, followed by a restoration to parental levels at the later phase of infection (Fig. 7A and B). Parental infection profiles were observed with the complemented strain Ox-*Rv1258c*. The attenuation pattern observed in both resting and activated macrophages suggests that *Rv1258c* plays a role in *M. tuberculosis* survival regardless of the macrophage activation status. Furthermore, the transient nature of the attenuated phenotype supports that *Rv1258c* plays a critical role during the initial phase of infection. To further demonstrate the relevance of our observations, infection profiles of the WT, Δ*Rv1258c*, and Ox-*Rv1258c* strains were determined in human monocyte-like THP-1 cells that were activated by retinoic acid and vitamin D_3 prior to

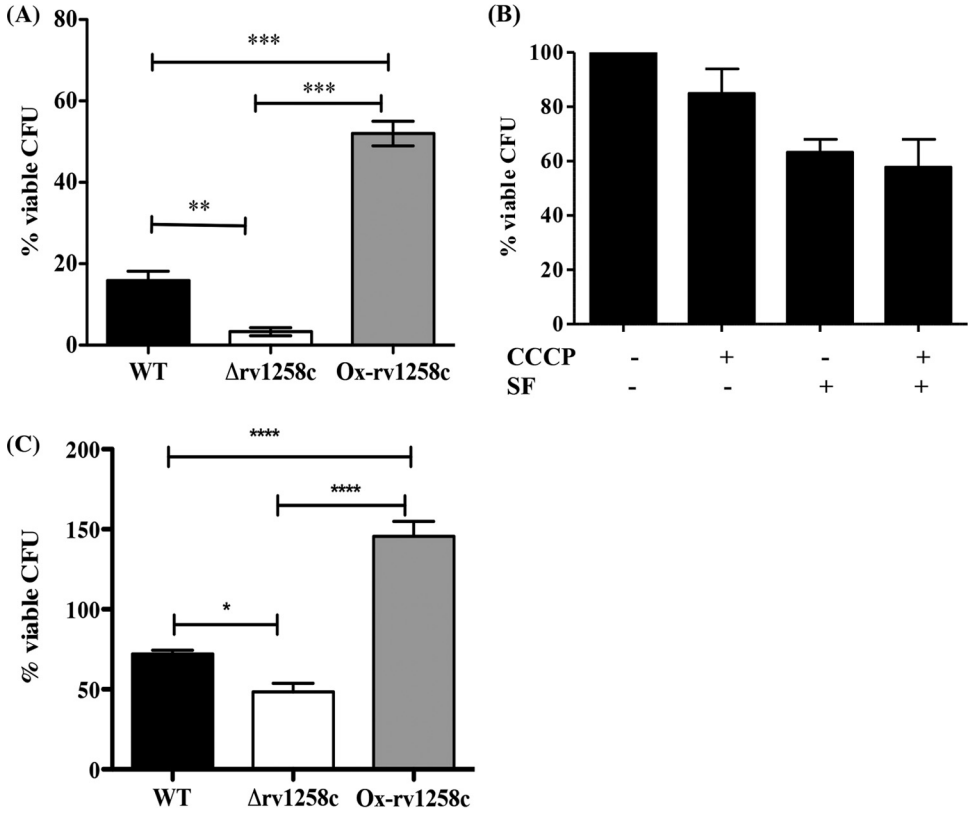

FIG 8 Susceptibility of Δ*Rv1258c* and Ox-*Rv1258c* strains to SF and human antimicrobial peptides. (A) Mid-log-phase cultures of *M. tuberculosis* parental (WT), Δ*Rv1258c*, and Ox-*Rv1258c* (complemented) strains were coincubated with 37 μg/ml SF for 24 h. (B) Mid-log-phase culture of the Δ*Rv1258c* strain was coincubated with 37 μg/ml SF for 24 h and 1 μg/ml CCCP. (C) WT, Δ*Rv1258c*, and Ox-*Rv1258c* strains were coincubated with LL-37 at 30 μg/ml for 72 h. The bacterial suspensions were then plated on 7H11, and CFU were determined after incubation at 37°C for 3 weeks. Data are expressed as the percentage of viable CFU when incubated in respective assay buffers (SF buffer and 0.1% acetic acid for LL-37). Data are the means ± SD from triplicates and are representative of two independent experiments. *, $P < 0.05$; **, $P < 0.01$; ***, $P < 0.001$; ****, $P < 0.0001$.

infection (34). Similar to the BMMO infection profile, an initial drop in viability was observed with the Δ*Rv1258c* strain at day 1 postinfection, but the bacilli's replicative ability was quickly restored from day 2 onwards, possibly reflecting a differential environmental pressure between murine and human macrophages (Fig. 7C). The complemented strain restored partially parental levels of growth.

To further examine the role of *Rv1258c* when *M. tuberculosis* encounters the lysosomal microenvironment, susceptibility to lysosomal SF killing was compared among WT, Δ*Rv1258c* mutant, and complemented strains. Incubation with 37 μg/ml SF for 24 h drastically reduced the viability of the Δ*Rv1258c* mutant to 3.3%, while the WT strain retained 17% viability (Fig. 8A). In contrast, Ox-*Rv1258c* exhibited greater resistance to SF killing than the WT, with 52% viability, correlating with the greater expression level of *Rv1258c* measured in the Ox-*Rv1258c* strain (Fig. 8A). Our results support a role for *Rv1258c* in *M. tuberculosis* survival during exposure to the lysosomal content. Previous literature proposed that the Tap efflux pump activity helps mycobacteria cope with the hostile environment by pumping out host-derived antimicrobial molecules (84–86). To test whether the Tap efflux pump activity is involved in the *M. tuberculosis* response to SF killing, the Ox-*Rv1258c* strain was incubated with SF in the presence of the proton motive force inhibitor CCCP. Since the Tap efflux pump requires energy to function, the presence of CCCP is expected to abrogate its activity. We observed that resistance to SF killing was comparable to that obtained in the absence of CCCP (Fig. 8B). In contrast, the enhanced resistance to streptomycin of Ox-*Rv1258c* was abrogated in the presence of CCCP, confirming the functionality of the Tap efflux pump in this *M. tuberculosis* strain (Table 4). Together, these data suggest that the mechanism(s) by which *Rv1258c*-encoded Tap is involved in *M. tuberculosis* resistance to lysosomal killing does not rely on its efflux pump activity. Mycobacterial efflux pumps have been described as part of the coupled biosynthesis/export machinery for mycobacterial cell wall components, and their respective mutants displayed defective growth in macrophage and mouse models (87). One could speculate that the absence of membrane-associ-

TABLE 4 Susceptibility of *M. tuberculosis* WT and Ox-*Rv1258c* strains to streptomycin

Treatment	MIC[a] (μg/ml)	
	WT	Ox-*Rv1258c* strain
Streptomycin	0.3	3.7
Streptomycin + CCCP	0.5	0.8

[a] The MIC of streptomycin was assayed over a range of 2-fold dilutions of the compound and in the presence or absence of 1 μg/ml CCCP. Data shown are representative of two independent experiments.

ated Tap in *M. tuberculosis* results in altered cell wall composition that may render the bacterium more permeable/vulnerable to antimicrobial compounds and compromise its cell wall-associated virulence, thereby impairing survival of this pathogen within its mammalian cell host.

Previous work suggested that ubiquitin-derived peptides isolated from murine lysosomes were involved in SF killing activity against *M. tuberculosis* (27). Other studies have pointed at the antimycobactericidal activity of other lysosomal small molecules, including LL-37, a multifunctional peptide belonging to the cathelicidin family and one of the most abundant antimicrobial molecules produced in various human host cells for *M. tuberculosis*, including lung epithelial cells, neutrophils, and macrophages (88, 89). To extend our observations to the human context, we assessed the susceptibility of WT, Δ*Rv1258c*, and Ox-*Rv1258c* strains to LL-37. Similar to observations made with the murine lysosomal SF, the Δ*Rv1258c* mutant exhibited greater susceptibility than its parental counterpart when incubated with 30 μg/ml of LL-37 for 72 h. In contrast, susceptibility of the Ox-*Rv1258c* strain was greater than that of the control bacteria (buffer only), suggesting a growth advantage conferred by *Rv1258c* overexpression in the presence of the antimicrobial peptide (Fig. 8C). Thus, these findings strongly suggest that (i) lysosomal killing of *M. tuberculosis* is likely mediated by several antimicrobial molecules and (ii) the mechanism by which Rv1258c is involved in *M. tuberculosis* resistance to lysosomal killing is not specific to one particular antimicrobial molecule. This notion fits well with the hypothesis that the absence of membrane-associated Tap renders the cell wall more vulnerable to antimicrobial peptide attack.

Conclusions. The lysosome is the major digestive organelle, with a critical role at the end of the endocytic pathway in mammalian cells (90). Its lumen contains more than 50 acid hydrolases, including proteases, peptidases, phosphatases, nucleases, glycosidases, sulfatases, and lipases, and it is maintained at an acidic pH necessary for the optimal activity of these enzymes to degrade all types of macromolecules (90). Under conditions that induce autophagy, short-length peptides such as ubiquitin-derived peptides and human cathelicidin h-CAP-18/LL-37 have also been shown to accumulate in lysosomal and autophagosomal structures, respectively, in a macrophage (27, 83). In addition to nitro-oxidative, nutrient-limiting, and hypoxic stresses within the macrophage, the antimycobacterial activity of these peptides becomes efficacious on intramacrophage *M. tuberculosis* when its phagosome either fuses with lysosomes or colocalizes with autophagosomes, which is also designated for degradation through lysosomal fusion (90). It is undeniable that the lysosomal environment is one of the intracellular microenvironments encountered by *M. tuberculosis* during macrophage infection.

This work increases our knowledge of the possible adaptive strategies devised by *M. tuberculosis* to resist the hostile lysosomal microenvironment. It complements previous transcriptome studies with the common aim of deciphering the mechanisms involved in the survival of *M. tuberculosis* inside its host macrophage.

ACKNOWLEDGMENTS

We gratefully acknowledge the Novartis Institute for Tropical Diseases for their generosity in providing the *M. tuberculosis* CDC1551 parental strain for our study. We also thank the Genome Technology Biology team at GIS for their sequencing efforts and assistance in computational analysis and for providing their valuable high-throughput computing resources.

This work was supported by the Singapore-MIT Alliance Infectious Disease Interdisciplinary Research Group (SMART-ID-IRG).

The funders had no role in study design, data collection and interpretation, or the decision to submit the work for publication. We have no conflicts of interest to declare.

REFERENCES

1. **Honer zu Bentrup K, Russell DG.** 2001. Mycobacterial persistence: adaptation to a changing environment. Trends Microbiol **9:**597–605. http://dx.doi.org/10.1016/S0966-842X(01)02238-7.
2. **Tsai MC, Chakravarty S, Zhu G, Xu J, Tanaka K, Koch C, Tufariello J, Flynn J, Chan J.** 2006. Characterization of the tuberculous granuloma in murine and human lungs: cellular composition and relative tissue oxygen tension. Cell Microbiol **8:**218–232. http://dx.doi.org/10.1111/j.1462-5822.2005.00612.x.
3. **Peyron P, Vaubourgeix J, Poquet Y, Levillain F, Botanch C, Bardou F, Daffe M, Emile JF, Marchou B, Cardona PJ, de Chastellier C, Altare F.** 2008. Foamy macrophages from tuberculous patients' granulomas constitute a nutrient-rich reservoir for M. tuberculosis persistence. PLoS Pathog **4:**e1000204. http://dx.doi.org/10.1371/journal.ppat.1000204.
4. **Aderem A, Underhill DM.** 1999. Mechanisms of phagocytosis in macrophages. Annu Rev Immunol **17:**593–623. http://dx.doi.org/10.1146/annurev.immunol.17.1.593.
5. **Weiss G, Schaible UE.** 2015. Macrophage defense mechanisms against intracellular bacteria. Immunol Rev **264:**182–203. http://dx.doi.org/10.1111/imr.12266.
6. **Cambier CJ, Falkow S, Ramakrishnan L.** 2014. Host evasion and exploitation schemes of *Mycobacterium tuberculosis*. Cell **159:**1497–1509. http://dx.doi.org/10.1016/j.cell.2014.11.024.
7. **Schaible UE, Sturgill-Koszycki S, Schlesinger PH, Russell DG.** 1998. Cytokine activation leads to acidification and increases maturation of *Mycobacterium avium*-containing phagosomes in murine macrophages. J Immunol **160:**1290–1296.
8. **MacMicking JD, Taylor GA, McKinney JD.** 2003. Immune control of tuberculosis by IFN-gamma-inducible LRG-47. Science **302:**654–659. http://dx.doi.org/10.1126/science.1088063.
9. **Ehrt S, Rhee K, Schnappinger D.** 2015. Mycobacterial genes essential for the pathogen's survival in the host. Immunol Rev **264:**319–326. http://dx.doi.org/10.1111/imr.12256.
10. **Homolka S, Niemann S, Russell DG, Rohde KH.** 2010. Functional genetic diversity among *Mycobacterium tuberculosis* complex clinical isolates: delineation of conserved core and lineage-specific transcriptomes during intracellular survival. PLoS Pathog **6:**e1000988. http://dx.doi.org/10.1371/journal.ppat.1000988.
11. **Schnappinger D, Ehrt S, Voskuil MI, Liu Y, Mangan JA, Monahan IM, Dolganov G, Efron B, Butcher PD, Nathan C, Schoolnik GK.** 2003. Transcriptional adaptation of *Mycobacterium tuberculosis* within macrophages: insights into the phagosomal environment. J Exp Med **198:**693–704. http://dx.doi.org/10.1084/jem.20030846.
12. **Rohde KH, Abramovitch RB, Russell DG.** 2007. *Mycobacterium tuberculosis* invasion of macrophages: linking bacterial gene expression to environmental cues. Cell Host Microbe **2:**352–364. http://dx.doi.org/10.1016/j.chom.2007.09.006.
13. **Fontan P, Aris V, Ghanny S, Soteropoulos P, Smith I.** 2008. Global transcriptional profile of *Mycobacterium tuberculosis* during THP-1 human macrophage infection. Infect Immun **76:**717–725. http://dx.doi.org/10.1128/IAI.00974-07.
14. **Cappelli G, Volpe E, Grassi M, Liseo B, Colizzi V, Mariani F.** 2006. Profiling of *Mycobacterium tuberculosis* gene expression during human macrophage infection: upregulation of the alternative sigma factor G, a group of transcriptional regulators, and proteins with unknown function. Res Microbiol **157:**445–455. http://dx.doi.org/10.1016/j.resmic.2005.10.007.
15. **Tailleux L, Waddell SJ, Pelizzola M, Mortellaro A, Withers M, Tanne A, Castagnoli PR, Gicquel B, Stoker NG, Butcher PD, Foti M, Neyrolles O.** 2008. Probing host pathogen cross-talk by transcriptional profiling of both *Mycobacterium tuberculosis* and infected human dendritic cells and macrophages. PLoS One **3:**e1403. http://dx.doi.org/10.1371/journal.pone.0001403.
16. **Bacon J, James BW, Wernisch L, Williams A, Morley KA, Hatch GJ, Mangan JA, Hinds J, Stoker NG, Butcher PD, Marsh PD.** 2004. The influence of reduced oxygen availability on pathogenicity and gene ex-

pression in *Mycobacterium tuberculosis*. Tuberculosis (Edinb) **84:**205–217. http://dx.doi.org/10.1016/j.tube.2003.12.011.
17. **Voskuil MI, Schnappinger D, Visconti KC, Harrell MI, Dolganov GM, Sherman DR, Schoolnik GK.** 2003. Inhibition of respiration by nitric oxide induces a *Mycobacterium tuberculosis* dormancy program. J Exp Med **198:**705–713. http://dx.doi.org/10.1084/jem.20030205.
18. **Ohno H, Zhu G, Mohan VP, Chu D, Kohno S, Jacobs WR, Chan J.** 2003. The effects of reactive nitrogen intermediates on gene expression in *Mycobacterium tuberculosis*. Cell Microbiol **5:**637–648. http://dx.doi.org/10.1046/j.1462-5822.2003.00307.x.
19. **Rodriguez GM, Voskuil MI, Gold B, Schoolnik GK, Smith I.** 2002. ideR, An essential gene in Mycobacterium tuberculosis: role of IdeR in iron-dependent gene expression, iron metabolism, and oxidative stress response. Infect Immun **70:**3371–3381. http://dx.doi.org/10.1128/IAI.70.7.3371-3381.2002.
20. **Fisher MA, Plikaytis BB, Shinnick TM.** 2002. Microarray analysis of the *Mycobacterium tuberculosis* transcriptional response to the acidic conditions found in phagosomes. J Bacteriol **184:**4025–4032. http://dx.doi.org/10.1128/JB.184.14.4025-4032.2002.
21. **Muttucumaru DG, Roberts G, Hinds J, Stabler RA, Parish T.** 2004. Gene expression profile of *Mycobacterium tuberculosis* in a nonreplicating state. Tuberculosis (Edinb) **84:**239–246. http://dx.doi.org/10.1016/j.tube.2003.12.006.
22. **Rustad TR, Harrell MI, Liao R, Sherman DR.** 2008. The enduring hypoxic response of *Mycobacterium tuberculosis*. PLoS One **3:**e1502. http://dx.doi.org/10.1371/journal.pone.0001502.
23. **Hampshire T, Soneji S, Bacon J, James BW, Hinds J, Laing K, Stabler RA, Marsh PD, Butcher PD.** 2004. Stationary phase gene expression of *Mycobacterium tuberculosis* following a progressive nutrient depletion: a model for persistent organisms? Tuberculosis (Edinb) **84:**228–238. http://dx.doi.org/10.1016/j.tube.2003.12.010.
24. **Betts JC, Lukey PT, Robb LC, McAdam RA, Duncan K.** 2002. Evaluation of a nutrient starvation model of *Mycobacterium tuberculosis* persistence by gene and protein expression profiling. Mol Microbiol **43:**717–731. http://dx.doi.org/10.1046/j.1365-2958.2002.02779.x.
25. **Keren I, Minami S, Rubin E, Lewis K.** 2011. Characterization and transcriptome analysis of Mycobacterium tuberculosis persisters. mBio **2:**e00100-11.
26. **Voskuil MI.** 2004. *Mycobacterium tuberculosis* gene expression during environmental conditions associated with latency. Tuberculosis (Edinb) **84:**138–143. http://dx.doi.org/10.1016/j.tube.2003.12.008.
27. **Alonso S, Pethe K, Russell DG, Purdy GE.** 2007. Lysosomal killing of *Mycobacterium* mediated by ubiquitin-derived peptides is enhanced by autophagy. Proc Natl Acad Sci U S A **104:**6031–6036. http://dx.doi.org/10.1073/pnas.0700036104.
28. **Huang DW, Sherman BT, Lempicki RA.** 2009. Systematic and integrative analysis of large gene lists using DAVID bioinformatics resources. Nat Protoc **4:**44–57.
29. **Edgar R, Domrachev M, Lash AE.** 2002. Gene Expression Omnibus: NCBI gene expression and hybridization array data repository. Nucleic Acids Res **30:**207–210. http://dx.doi.org/10.1093/nar/30.1.207.
30. **Rohde KH, Veiga DFT, Caldwell S, Balázsi G, Russell DG.** 2012. Linking the transcriptional profiles and the physiological states of *Mycobacterium tuberculosis* during an extended intracellular infection. PLoS Pathog **8:**e1002769. http://dx.doi.org/10.1371/journal.ppat.1002769.
31. **Bardarov S, Bardarov S, Jr, Pavelka MS, Jr, Sambandamurthy V, Larsen M, Tufariello J, Chan J, Hatfull G, Jacobs WR, Jr.** 2002. Specialized transduction: an efficient method for generating marked and unmarked targeted gene disruptions in *Mycobacterium tuberculosis*, *M. bovis* BCG and *M. smegmatis*. Microbiology **148:**3007–3017. http://dx.doi.org/10.1099/00221287-148-10-3007.
32. **Parish T, Stoker NG.** 2000. Use of a flexible cassette method to generate a double unmarked *Mycobacterium tuberculosis* tlyA plcABC mutant by gene replacement. Microbiology **146**(Part 8)**:**1969–1975. http://dx.doi.org/10.1099/00221287-146-8-1969.
33. **Stover CK, de la Cruz VF, Fuerst TR, Burlein JE, Benson LA, Bennett LT, Bansal GP, Young JF, Lee MH, Hatfull GF, Snapper SB, Barletta RG, Jacobs WR, Jr, Bloom BR.** 1991. New use of BCG for recombinant vaccines. Nature **351:**456–460. http://dx.doi.org/10.1038/351456a0.
34. **Estrella J, Kan-Sutton C, Gong K, Eissa TN, Rajagopalan M, Lewis D, Hunter R, Jagannath C.** 2011. A novel in vitro human macrophage model to study the persistence of *Mycobacterium tuberculosis* using Vitamin D and retinoic acid activated THP-1 macrophages. Front Microbiol **2:**67–74.
35. **Wayne LG, Hayes LG.** 1996. An in vitro model for sequential study of shiftdown of *Mycobacterium tuberculosis* through two stages of nonreplicating persistence. Infect Immun **64:**2062–2069.
36. **Loebel RO, Shorr E, Richardson HB.** 1933. The influence of adverse conditions upon the respiratory metabolism and growth of human tubercle bacilli. J Bacteriol **26:**167–200.
37. **Stewart GR, Wernisch L, Stabler R, Mangan JA, Hinds J, Laing KG, Young DB, Butcher PD.** 2002. Dissection of the heat-shock response in *Mycobacterium tuberculosis* using mutants and microarrays. Microbiology **148:**3129–3138. http://dx.doi.org/10.1099/00221287-148-10-3129.
38. **Rachman H, Strong M, Ulrichs T, Grode L, Schuchhardt J, Mollenkopf H, Kosmiadi GA, Eisenberg D, Kaufmann SHE.** 2006. Unique transcriptome signature of *Mycobacterium tuberculosis* in pulmonary tuberculosis. Infect Immun **74:**1233–1242. http://dx.doi.org/10.1128/IAI.74.2.1233-1242.2006.
39. **Kress W, Maglica Ž, Weber-Ban E.** 2009. Clp chaperone-proteases: structure and function. Res Microbiol **160:**618–628. http://dx.doi.org/10.1016/j.resmic.2009.08.006.
40. **Roberts DM, Personne Y, Ollinger J, Parish T.** 2013. Proteases in *Mycobacterium tuberculosis* pathogenesis: potential as drug targets. Future Microbiol **8:**621–631. http://dx.doi.org/10.2217/fmb.13.25.
41. **Moreira W, Ngan GJY, Low JL, Poulsen A, Chia BCS, Ang MJY, Yap A, Fulwood J, Lakshmanan U, Lim J, Khoo AYT, Flotow H, Hill J, Raju RM, Rubin EJ, Dick T.** 2015. Target mechanism-based whole-cell screening identifies Bortezomib as an inhibitor of caseinolytic protease in mycobacteria. mBio **6:**e00253.
42. **Talaat AM, Lyons R, Howard ST, Johnston SA.** 2004. The temporal expression profile of *Mycobacterium tuberculosis* infection in mice. Proc Natl Acad Sci U S A **101:**4602–4607. http://dx.doi.org/10.1073/pnas.0306023101.
43. **Munoz-Elias EJ, Upton AM, Cherian J, McKinney JD.** 2006. Role of the methylcitrate cycle in *Mycobacterium tuberculosis* metabolism, intracellular growth, and virulence. Mol Microbiol **60:**1109–1122. http://dx.doi.org/10.1111/j.1365-2958.2006.05155.x.
44. **Gould TA, van de Langemheen H, Munoz-Elias EJ, McKinney JD, Sacchettini JC.** 2006. Dual role of isocitrate lyase 1 in the glyoxylate and methylcitrate cycles in *Mycobacterium tuberculosis*. Mol Microbiol **61:**940–947. http://dx.doi.org/10.1111/j.1365-2958.2006.05297.x.
45. **Bacon J, Alderwick LJ, Allnutt JA, Gabasova E, Watson R, Hatch KA, Clark SO, Jeeves RE, Marriott A, Rayner E, Tolley H, Pearson G, Hall G, Besra GS, Wernisch L, Williams A, Marsh PD.** 2014. Non-replicating Mycobacterium tuberculosis elicits a reduced infectivity profile with corresponding modifications to the cell wall and extracellular matrix. PLoS One **9:**e87329. http://dx.doi.org/10.1371/journal.pone.0087329.
46. **Yuan Y, Zhu Y, Crane DD, Barry CE, III.** 1998. The effect of oxygenated mycolic acid composition on cell wall function and macrophage growth in Mycobacterium tuberculosis. Mol Microbiol **29:**1449–1458. http://dx.doi.org/10.1046/j.1365-2958.1998.01026.x.
47. **Sirakova TD, Thirumala AK, Dubey VS, Sprecher H, Kolattukudy PE.** 2001. The *Mycobacterium tuberculosis pks2* gene encodes the synthase for the hepta- and octamethyl-branched fatty acids required for sulfolipid synthesis. J Biol Chem **276:**16833–16839. http://dx.doi.org/10.1074/jbc.M011468200.
48. **Phetsuksiri B, Jackson M, Scherman H, McNeil M, Besra GS, Baulard AR, Slayden RA, DeBarber AE, Barry CE, Baird MS, Crick DC, Brennan PJ.** 2003. Unique mechanism of action of the thiourea drug isoxyl on *Mycobacterium tuberculosis*. J Biol Chem **278:**53123–53130. http://dx.doi.org/10.1074/jbc.M311209200.
49. **Cantrell S, Leavell M, Marjanovic O, Iavarone A, Leary J, Riley L.** 2013. Free mycolic acid accumulation in the cell wall of the *mce1* operon mutant strain of *Mycobacterium tuberculosis*. J Microbiol **51:**619–626. http://dx.doi.org/10.1007/s12275-013-3092-y.
50. **Shimono N, Morici L, Casali N, Cantrell S, Sidders B, Ehrt S, Riley LW.** 2003. Hypervirulent mutant of *Mycobacterium tuberculosis* resulting from disruption of the *mce1* operon. Proc Natl Acad Sci U S A **100:**15918–15923. http://dx.doi.org/10.1073/pnas.2433882100.
51. **Ojha AK, Baughn AD, Sambandan D, Hsu T, Trivelli X, Guerardel Y, Alahari A, Kremer L, Jacobs WR, Hatfull GF.** 2008. Growth of *Mycobacterium tuberculosis* biofilms containing free mycolic acids and harbouring drug-tolerant bacteria. Mol Microbiol **69:**164–174. http://dx.doi.org/10.1111/j.1365-2958.2008.06274.x.
52. **Esparza M, Palomares B, García T, Espinosa P, Zenteno E, Mancilla R.** 2015. PstS-1, the 38-kDa *Mycobacterium tuberculosis* glycoprotein, is an

adhesin which binds the macrophage mannose receptor and promotes phagocytosis. Scand J Immunol **81:**46–55. http://dx.doi.org/10.1111/sji.12249.

53. **Park H-D, Guinn KM, Harrell MI, Liao R, Voskuil MI, Tompa M, Schoolnik GK, Sherman DR.** 2003. Rv3133c/dosR is a transcription factor that mediates the hypoxic response of *Mycobacterium tuberculosis*. Mol Microbiol **48:**833–843. http://dx.doi.org/10.1046/j.1365-2958.2003.03474.x.
54. **Via LE, Lin PL, Ray SM, Carrillo J, Allen SS, Eum SY, Taylor K, Klein E, Manjunatha U, Gonzales J, Lee EG, Park SK, Raleigh JA, Cho SN, McMurray DN, Flynn JL, Barry CE.** 2008. Tuberculous granulomas are hypoxic in guinea pigs, rabbits, and nonhuman primates. Infect Immun **76:**2333–2340. http://dx.doi.org/10.1128/IAI.01515-07.
55. **Ehrt S, Schnappinger D.** 2009. Mycobacterial survival strategies in the phagosome: defence against host stresses. Cell Microbiol **11:**1170–1178. http://dx.doi.org/10.1111/j.1462-5822.2009.01335.x.
56. **Kendall SL, Movahedzadeh F, Rison SC, Wernisch L, Parish T, Duncan K, Betts JC, Stoker NG.** 2004. The *Mycobacterium tuberculosis* dosRS two-component system is induced by multiple stresses. Tuberculosis (Edinb) **84:**247–255. http://dx.doi.org/10.1016/j.tube.2003.12.007.
57. **Brodin P, Rosenkrands I, Andersen P, Cole ST, Brosch R.** 2004. ESAT-6 proteins: protective antigens and virulence factors? Trends Microbiol **12:**500–508. http://dx.doi.org/10.1016/j.tim.2004.09.007.
58. **Li W, Deng G, Li M, Zeng J, Zhao L, Liu X, Wang Y.** 2014. A recombinant adenovirus expressing CFP10, ESAT6, Ag85A and Ag85B of Mycobacterium tuberculosis elicits strong antigen-specific immune responses in mice. Mol Immunol **62:**86–95. http://dx.doi.org/10.1016/j.molimm.2014.06.007.
59. **Chen W, Bao Y, Chen X, Burton J, Gong X, Gu D, Mi Y, Bao L.** 2016. *Mycobacterium tuberculosis* PE25/PPE41 protein complex induces activation and maturation of dendritic cells and drives Th2-biased immune responses. Med Microbiol Immunol **205:**119–131. http://dx.doi.org/10.1007/s00430-015-0434-x.
60. **Li G, Liu G, Song N, Kong C, Huang Q, Su H, Bi A, Luo L, Zhu L, Xu Y, Wang H.** 2015. A novel recombinant BCG-expressing pro-apoptotic protein BAX enhances Th1 protective immune responses in mice. Mol Immunol **66:**346–356. http://dx.doi.org/10.1016/j.molimm.2015.04.003.
61. **Ng VH, Cox JS, Sousa AO, MacMicking JD, McKinney JD.** 2004. Role of KatG catalase-peroxidase in mycobacterial pathogenesis: countering the phagocyte oxidative burst. Mol Microbiol **52:**1291–1302. http://dx.doi.org/10.1111/j.1365-2958.2004.04078.x.
62. **Master SS, Springer B, Sander P, Boettger EC, Deretic V, Timmins GS.** 2002. Oxidative stress response genes in *Mycobacterium tuberculosis*: role of ahpC in resistance to peroxynitrite and stage-specific survival in macrophages. Microbiology **148:**3139–3144. http://dx.doi.org/10.1099/00221287-148-10-3139.
63. **Hillas PJ, del Alba FS, Oyarzabal J, Wilks A, Ortiz de Montellano PR.** 2000. The AhpC and AhpD antioxidant defense system of *Mycobacterium tuberculosis*. J Biol Chem **275:**18801–18809. http://dx.doi.org/10.1074/jbc.M001001200.
64. **Huet G, Daffé M, Saves I.** 2005. Identification of the *Mycobacterium tuberculosis* SUF machinery as the exclusive mycobacterial system of [Fe-S] cluster assembly: evidence for its implication in the pathogen's survival. J Bacteriol **187:**6137–6146. http://dx.doi.org/10.1128/JB.187.17.6137-6146.2005.
65. **Shi L, Sohaskey CD, Kana BD, Dawes S, North RJ, Mizrahi V, Gennaro ML.** 2005. Changes in energy metabolism of *Mycobacterium tuberculosis* in mouse lung and under in vitro conditions affecting aerobic respiration. Proc Natl Acad Sci U S A **102:**15629–15634. http://dx.doi.org/10.1073/pnas.0507850102.
66. **Watanabe S, Zimmermann M, Goodwin MB, Sauer U, Barry CE, III, Boshoff HI.** 2011. Fumarate reductase activity maintains an energized membrane in anaerobic Mycobacterium tuberculosis. PLoS Pathog **7:**e1002287. http://dx.doi.org/10.1371/journal.ppat.1002287.
67. **Beste DJV, Laing E, Bonde B, Avignone-Rossa C, Bushell ME, McFadden JJ.** 2007. Transcriptomic analysis identifies growth rate modulation as a component of the adaptation of mycobacteria to survival inside the macrophage. J Bacteriol **189:**3969–3976. http://dx.doi.org/10.1128/JB.01787-06.
68. **Albrethsen J, Agner J, Piersma SR, Hojrup P, Pham TV, Weldingh K, Jimenez CR, Andersen P, Rosenkrands I.** 2013. Proteomic profiling of *Mycobacterium tuberculosis* identifies nutrient-starvation-responsive toxin-antitoxin systems. Mol Cell Proteomics **12:**1180–1191. http://dx.doi.org/10.1074/mcp.M112.018846.
69. **Sherman DR, Voskuil M, Schnappinger D, Liao R, Harrell MI, Schoolnik GK.** 2001. Regulation of the *Mycobacterium tuberculosis* hypoxic response gene encoding α-crystallin. Proc Natl Acad Sci U S A **98:**7534–7539. http://dx.doi.org/10.1073/pnas.121172498.
70. **Morris RP, Nguyen L, Gatfield J, Visconti K, Nguyen K, Schnappinger D, Ehrt S, Liu Y, Heifets L, Pieters J, Schoolnik G, Thompson CJ.** 2005. Ancestral antibiotic resistance in *Mycobacterium tuberculosis*. Proc Natl Acad Sci U S A **102:**12200–12205. http://dx.doi.org/10.1073/pnas.0505446102.
71. **Adams Kristin N, Takaki K, Connolly Lynn E, Wiedenhoft H, Winglee K, Humbert O, Edelstein Paul H, Cosma Christine L, Ramakrishnan L.** 2011. Drug tolerance in replicating mycobacteria mediated by a macrophage-induced efflux mechanism. Cell **145:**39–53. http://dx.doi.org/10.1016/j.cell.2011.02.022.
72. **Madsen CT, Jakobsen L, Buriankova K, Doucet-Populaire F, Pernodet JL, Douthwaite S.** 2005. Methyltransferase Erm(37) slips on rRNA to confer atypical resistance in *Mycobacterium tuberculosis*. J Biol Chem **280:**38942–38947. http://dx.doi.org/10.1074/jbc.M505727200.
73. **Chen W, Biswas T, Porter VR, Tsodikov OV, Garneau-Tsodikova S.** 2011. Unusual regioversatility of acetyltransferase Eis, a cause of drug resistance in XDR-TB. Proc Natl Acad Sci U S A **108:**9804–9808. http://dx.doi.org/10.1073/pnas.1105379108.
74. **Geiman DE, Raghunand TR, Agarwal N, Bishai WR.** 2006. Differential gene expression in response to exposure to antimycobacterial agents and other stress conditions among seven *Mycobacterium tuberculosis* whiB-like genes. Antimicrob Agents Chemother **50:**2836–2841. http://dx.doi.org/10.1128/AAC.00295-06.
75. **Larsson C, Luna B, Ammerman NC, Maiga M, Agarwal N, Bishai WR.** 2012. Gene expression of *Mycobacterium tuberculosis* putative transcription factors whiB1-7 in redox environments. PLoS One **7:**e37516. http://dx.doi.org/10.1371/journal.pone.0037516.
76. **Kana BD, Gordhan BG, Downing KJ, Sung N, Vostroktunova G, Machowski EE, Tsenova L, Young M, Kaprelyants A, Kaplan G, Mizrahi V.** 2008. The resuscitation-promoting factors of Mycobacterium tuberculosis are required for virulence and resuscitation from dormancy but are collectively dispensable for growth in vitro. Mol Microbiol **67:**672–684. http://dx.doi.org/10.1111/j.1365-2958.2007.06078.x.
77. **Kalscheuer R, Syson K, Veeraraghavan U, Weinrick B, Biermann KE, Liu Z, Sacchettini JC, Besra G, Bornemann S, Jacobs WR.** 2010. Self-poisoning of *Mycobacterium tuberculosis* by targeting GlgE in an alpha-glucan pathway. Nat Chem Biol **6:**376–384. http://dx.doi.org/10.1038/nchembio.340.
78. **Arcus VL, Rainey PB, Turner SJ.** 2005. The PIN-domain toxin–antitoxin array in mycobacteria. Trends Microbiol **13:**360–365. http://dx.doi.org/10.1016/j.tim.2005.06.008.
79. **Brzozowska I, Zielenkiewicz U.** 2013. Regulation of toxin–antitoxin systems by proteolysis. Plasmid **70:**33–41. http://dx.doi.org/10.1016/j.plasmid.2013.01.007.
80. **Yamaguchi Y, Park J-H, Inouye M.** 2011. Toxin-antitoxin systems in Bacteria and Archaea. Annu Rev Genet **45:**61–79. http://dx.doi.org/10.1146/annurev-genet-110410-132412.
81. **Ahidjo BA, Kuhnert D, McKenzie JL, Machowski EE, Gordhan BG, Arcus V, Abrahams GL, Mizrahi V.** 2011. VapC toxins from *Mycobacterium tuberculosis* are ribonucleases that differentially inhibit growth and are neutralized by cognate VapB antitoxins. PLoS One **6:**e21738. http://dx.doi.org/10.1371/journal.pone.0021738.
82. **Sutcliffe IC, Harrington DJ.** 2004. Lipoproteins of *Mycobacterium tuberculosis*: an abundant and functionally diverse class of cell envelope components. FEMS Microbiol Rev **28:**645–659. http://dx.doi.org/10.1016/j.femsre.2004.06.002.
83. **Abramovitch RB, Rohde KH, Hsu F-F, Russell DG.** 2011. aprABC: a *Mycobacterium tuberculosis* complex-specific locus that modulates pH-driven adaptation to the macrophage phagosome. Mol Microbiol **80:**678–694. http://dx.doi.org/10.1111/j.1365-2958.2011.07601.x.
84. **da Silva PEA, Von Groll A, Martin A, Palomino JC.** 2011. Efflux as a mechanism for drug resistance in *Mycobacterium tuberculosis*. FEMS Immunol Med Microbiol **63:**1–9. http://dx.doi.org/10.1111/j.1574-695X.2011.00831.x.
85. **Ramón-García S, Martín C, Aínsa JA, De Rossi E.** 2006. Characterization of tetracycline resistance mediated by the efflux pump Tap from

Mycobacterium fortuitum. J Antimicrob Chemother **57:**252–259. http://dx.doi.org/10.1093/jac/dki436.

86. **Ramón-García S, Mick V, Dainese E, Martín C, Thompson CJ, De Rossi E, Manganelli R, Aínsa JA.** 2012. Functional and genetic characterization of the Tap efflux pump in *Mycobacterium bovis* BCG. Antimicrob Agents Chemother **56:**2074–2083. http://dx.doi.org/10.1128/AAC.05946-11.
87. **Jain M, Cox JS.** 2005. Interaction between polyketide synthase and transporter suggests coupled synthesis and export of virulence lipid in *M. tuberculosis*. PLoS Pathog **1:**e2. http://dx.doi.org/10.1371/journal.ppat.0010002.
88. **Chingaté S, Delgado G, Salazar LM, Soto CY.** 2015. The ATPase activity of the mycobacterial plasma membrane is inhibited by the LL37-analogous peptide LLAP. Peptides **71:**222–228. http://dx.doi.org/10.1016/j.peptides.2015.07.021.
89. **Rivas-Santiago B, Hernandez-Pando R, Carranza C, Juarez E, Contreras JL, Aguilar-Leon D, Torres M, Sada E.** 2008. Expression of cathelicidin LL-37 during *Mycobacterium tuberculosis* infection in human alveolar macrophages, monocytes, neutrophils, and epithelial cells. Infect Immun **76:**935–941. http://dx.doi.org/10.1128/IAI.01218-07.
90. **Lübke T, Lobel P, Sleat DE.** 2009. Proteomics of the lysosome. Biochim Biophys Acta **1793:**625–635. http://dx.doi.org/10.1016/j.bbamcr.2008.09.018.